Behavioural Brain Research 295 (2015) 45–63

Contents lists available at ScienceDirect

Behavioural Brain Research

journal homepage: www.elsevier.com/locate/bbr

Research report

Distribution of serotonin 5-HT$_{1A}$-binding sites in the brainstem and the hypothalamus, and their roles in 5-HT-induced sleep and ingestive behaviors in rock pigeons (*Columba livia*)

Tiago Souza dos Santos[a,1], Jéssica Krüger[a,1], Fernando Falkenburger Melleu[a,1], Christina Herold[d,3], Karl Zilles[f,g,h,4], Anicleto Poli[c,2], Onur Güntürkün[e,5], José Marino-Neto[a,b,*]

[a] *Department of Physiological Sciences, CCB, Federal University of Santa Catarina, 88040-900 Florianópolis, SC, Brazil*
[b] *Institute of Biomedical Engineering, EEL-CTC, Federal University of Santa Catarina, 88040-900 Florianópolis, SC, Brazil*
[c] *Department of Pharmacology, CCB, Federal University of Santa Catarina, 88040-900 Florianópolis, SC, Brazil*
[d] *C & O. Vogt Institute for Brain Research, Heinrich Heine University, 40225 Düsseldorf, Germany*
[e] *Institute for Cognitive Neuroscience, Faculty of Psychology, Ruhr University Bochum, 44780 Bochum, Germany*
[f] *Institute of Neuroscience and Medicine INM-1, Research Center Jülich, 52425 Jülich, Germany*
[g] *Department of Psychiatry, Psychotherapy and Psychosomatics, RWTH Aachen University, 52074 Aachen, Germany*
[h] *JARA – Translational Brain Medicine, 52074 Aachen, Germany*

HIGHLIGHTS

- 5-HT$_{1AR}$ was found in brainstem 5-HT areas and in the hypothalamus of pigeons.
- ICV 5-HT or DPAT evokes drinking, sleep, and c-Fos expression in these areas.
- 5-HT$_{1AR}$ heteroreceptor antagonist blocks 5-HT- and DPAT-evoked drinking and sleep.
- 5-HT-specific neurotoxin 5,7-DHT does not alter 5-HT activity but does increase sleep.
- 5-HT$_{1ARs}$ play crucial but complex roles in ingestive and postprandial behavior.

ARTICLE INFO

Article history:
Received 1 October 2014
Received in revised form 20 February 2015
Accepted 26 March 2015
Available online 3 April 2015

ABSTRACT

Serotonin 1A receptors (5-HT$_{1ARs}$), which are widely distributed in the mammalian brain, participate in cognitive and emotional functions. In birds, 5-HT$_{1ARs}$ are expressed in prosencephalic areas involved in visual and cognitive functions. Diverse evidence supports 5-HT$_{1AR}$-mediated 5-HT-induced ingestive and sleep behaviors in birds. Here, we describe the distribution of 5-HT$_{1ARs}$ in the hypothalamus and brainstem of birds, analyze their potential roles in sleep and ingestive behaviors, and attempt to determine

Abbreviations: A6, caudal part of locus coeruleus; A8, rostral part of locus coeruleus; AL, ansa lenticularis; AM, nucleus anterior medialis hypothalami; Anl, nucleus annularis; BC, brachium conjunctivum; BNSTl, bed nucleus of stria terminalis, pars lateral; CA, anterior commissure; CO, chiasma opticum; CP, posterior commissure; CS, nucleus centralis superior; DMN, nucleus dorsomedialis hypothalami; DSD, dorsal supraoptic decussation; DSV, ventral supraoptic decussation; FDB, fasciculus diagonalis brocae; FLM, fasciculus longitudinalis medialis; GCt, griseum centralis; IF, infundibular tract; IN, nucleus infundibuli; LC, nucleus linearis caudalis; LHy, lateral hypothalamic area; ML, nucleus mamillar lateralis; MM, nucleus mamillaris medialis; n.IV, nucleus trochlearis; n.V, nucleus principalis nervi trigemini; OM, occipitomesencephalic tract; PD, nucleus preopticus dorsalis; PLH, nucleus lateralis hypothalami posterioris; PMH, nucleus medialis hypothalami posterioris; PMM, nucleus pre-mamillaris; POA, nucleus preopticus anterior; POM, nucleus preopticus medialis; PPM, nucleus preopticus magnocellularis; PVNm, nucleus paraventricularis, pars magnocellularis; PVNp, nucleus paraventricularis, pars parvocellularis; PVO, paraventricular organ; QF, quinto frontalis tract; R, nucleus raphe pontis; RPO, nucleus reticularis pontis oralis; Rt, nucleus rotundus; ScD, nucleus subcoeruleus dorsalis; SCE, stratum cellulare externum; SCl, stratum cellulare internum; ScV, nucleus subcoeruleus ventralis; SFO, subfornical organ; SL, septal lateral nucleus; SOE, nucleus supraopticus externus; TSM, tractus septomesencephalicus; VMN, nucleus ventromedialis hypothalami; ZpFLM, zone peri-fasciculus longitudinalis medialis.

* Corresponding author at: Department of Physiological Sciences CCB, Federal University of Santa Catarina, 88040-900 Florianópolis, SC, Brazil. Tel.: +55 48 3721 8760; fax: +55 48 3331 8686.
E-mail addresses: santos.ts@hotmail.com (T.S. dos Santos), jessica.kkruger@hotmail.com (J. Krüger), fmelleu@gmail.com (F.F. Melleu), christina.herold@uni-duesseldorf.de (C. Herold), k.zilles@fz-juelich.de (K. Zilles), poli@ccb.ufsc.br (A. Poli), onur.guentuerkuen@ruhr-uni-bochum.de (O. Güntürkün), marino@ieb.ufsc.br, marino@ccb.ufsc.br (J. Marino-Neto).
[1] Tel.: +55 21 48 37218760.
[2] Tel.: +55 21 48 37214861.
[3] Tel.: +49 211 81 12666; fax: +49 211 81 12366.
[4] Tel.: +49 2461 613015.
[5] Address: Biopsychology, Institute of Cognitive Neuroscience, Faculty of Psychology, Ruhr-University Bochum, 44780 Bochum, Germany. Tel.: +49 234 3226213; fax: +49 234 3214377.

http://dx.doi.org/10.1016/j.bbr.2015.03.059

Keywords:
Serotonin
Sleep
Drinking
Feeding
5-HT-1A receptor
Cerebrospinal fluid

the involvement of auto-/hetero-5-HT_{1ARs} in these behaviors. In 6 pigeons, the anatomical distribution of [^{3}H]8-OH-DPAT binding in the rostral brainstem and hypothalamus was examined. Ingestive/sleep behaviors were recorded (1 h) in 16 pigeons pretreated with MM77 (a heterosynaptic 5-HT_{1AR} antagonist; 23 or 69 nmol) for 20 min, followed by intracerebroventricular ICV injection of 5-HT (N:8; 150 nmol), 8-OH-DPAT (DPAT, a 5-$HT_{1A,7R}$ agonist, 30 nmol N:8) or vehicle. 5-HT- and DPAT-induced sleep and ingestive behaviors, brainstem 5-HT neuronal density and brain 5-HT content were examined in 12 pigeons, pretreated by ICV with the 5-HT neurotoxin 5,7-dihydroxytryptamine (5,7-DHT) or vehicle (N:6/group). The distribution of brainstem and diencephalic c-Fos immunoreactivity after ICV injection of 5-HT, DPAT or vehicle (N:5/group) into birds provided with or denied access to water is also described. 5-HT_{1ARs} are concentrated in the brainstem 5-HTergic areas and throughout the periventricular hypothalamus, preoptic nuclei and circumventricular organs. 5-HT and DPAT produced a complex c-Fos expression pattern in the 5-HT_{1AR}-enriched preoptic hypothalamus and the circumventricular organs, which are related to drinking and sleep regulation, but modestly affected c-Fos expression in 5-HTergic neurons. The 5-HT-induced ingestivebehaviors and the 5-HT- and DPAT-induced sleep behaviors were reduced by MM77 pretreatment. 5,7-DHT increased sleep per se, decreased tryptophan hydroxylase expression in the raphe nuclei and decreased prosencephalic 5-HT release but failed to affect 5-HT- or DPAT-induced drinking or sleep behavior. 5-HT- and DPAT-induced ingestive and sleep behaviors in pigeons appear to be mediated by heterosynaptic and/or non-somatodendritic presynaptic 5-HT_{1ARs} localized to periventricular diencephalic circuits.

1. Introduction

Postprandial states in both mammals [1–3] and birds [4–6] are characterized by an increased incidence of grooming, drinking and resting. These behaviors, which occur in a relatively fixed temporal setting, constitute the so-called behavioral satiety sequence (BSS) in both classes of vertebrates. Additionally, BSS expression appears to be selectively affected by changes in serotonin (5-HT) neurotransmission in both vertebrate classes. Increased activity of 5-HT circuits exerts suppressive effects on food and water intake in mammals (e.g., [7]) and in pigeons [8–10]. Intracerebroventricular (ICV) injection of 5-HT in pigeons [9,11–13] evoked a sequence of hypophagia, drinking and sleep that parallels the BSS in pigeons [6]. On the other hand, increased feeding was observed in free-feeding pigeons after intra-hypothalamic and intra-amygdalar injection of a 5-$HT_{1/2}$ receptor antagonist or intra-raphe injection of 8-OH-DPAT (DPAT; a 5-$HT_{1A/7}$ receptor agonist) [14], indicating that5-HT afferents exert tonic inhibitory control on feeding-related prosencephalic circuits in free-feeding pigeons, similar to the findings in mammals.

Furthermore, increased activity of 5-HTergic circuits also exerts an inhibitory effect on sleep in both vertebrate classes [15,16,12,13]. Brainstem 5-HTergic neurons in mammals are active during waking but display reduced firing rates, and may not fire at all, during sleep states [17,15,18]. Activating 5-HT receptors via ICV injection of 5-HT evokes hypophagia and behavioral/electrographic sleep-like states in carnivores and rodents (e.g., [19]). Furthermore, in mammals, intra-raphe injection of DPAT increases sleep signs [20,21], indicating an important role of the presynaptic 5-HT_{1A} receptor subtype (5-HT_{1AR}) in decreasing the activity of 5-HT-related mechanisms that promote wakefulness in mammals [15,18]. ICV injection of DPAT into free-feeding pigeons at the identical ventricular regions to which 5-HT evokes the hypophagia/drinking/sleep sequence and increases feeding and drinking behaviors; these effects are followed by increased behavioral and electrographic signs of sleep [12,13]. Thus, it is possible that the activity of central 5-HT circuits may coordinate satiety processes, influencing the expression and sequential appearance of the major components of the mammalian and avian BSS.

The similarities between the effects of ICV-injected 5-HT and DPAT on behaviors in pigeons indicate a crucial role of 5-HT_{1ARs} in satiety-related circuits. Similar to mammals, systemic DPAT injection reduces serotonergic neurotransmission in pigeons [22–24,24], possibly by acting on inhibitory 5-HT_{1A} autoreceptor-mediated mechanisms, similar to those found in mammals. Accordingly, pretreatment with a 5-HT_{1AR} antagonist, such as WAY100635 decreases drinking and sleep behaviors induced by ICV 5-HT injection and antagonizes DPAT-induced feeding and drinking behaviors [13]. Furthermore, the density of c-Fos protein expression in midline and dorsal brainstem 5-HTergic cell populations double-labeled for tryptophan hydroxylase (TPH) was reduced in 5-HT (ICV)-injected pigeons compared to vehicle-injected animals. Moreover, the activity of these double-labeled neurons negatively correlated to sleep [12]. These data suggest that the drinking- and sleep-inducing effects of ICV 5-HT injection into pigeons result from the 5-HT-induced inhibition of 5-HTergic neurons (via activation of 5-HT_{1ARs}) [12,13]. Taken together, these results indicate a mechanistic hypothesis in which a feeding-evoked increase in ventricular 5-HT results in 5-HT-mediated hypophagia. This mechanism, subsequently, results in a 5-HT_{1AR}-mediated reduction in the activity of drinking- and sleep-inhibitory 5-HTergic neurons, thus favoring the post-prandial satiety-related appearance of these behaviors. In addition to the possible relevance of such mechanisms to coordinating BSS behavior in pigeons, these data also suggest that the roles and mechanisms of 5-HT represent shared, evolutionarily conserved functional attributes of the serotonergic circuits in the amniote brain.

However, before proceeding to a closer examination of the circumventricular, BSS-related functions of intraventricular 5-HTergic neurons, the hypothesis described above must be further tested on anatomical and pharmacological bases. In mammals, 5-HT_{1ARs} are localized to both synaptic terminals: as an autoreceptor that regulates serotonergic neuronal activity and as a heteroreceptor that modulates 5-HT-mediated effects via several serotonergic targets [25]. In mammalian brains, a high density of 5-HT_{1ARs} was detected in 5-HTergic areas of the brainstem [26] and the forebrain, such as the cingulate and entorhinal cortices, the hippocampus, the amygdala, the septum, the thalamus and the hypothalamus [27–32]. An autoradiographic study using pigeons indicated moderate to high expression of binding sites to [^{3}H]8-OH-DPAT in forebrain regions including the nidopallium, the hyperpallium, the hippocampus, the basal ganglia, and the amygdala [33]. However, the distribution of these receptors in the brainstem and in periventricular areas, such as the hypothalamus, of birds remains unknown.

Furthermore, the 5-HT_{1AR} antagonist used to examine these activities, WAY100635, acts at both pre- and postsynaptic 5-HT_{1ARs} [34,35], obscuring the localization of these receptors. A suitable

approach to assess these functions of 5-HT is pretreatment with a postsynaptic selective 5-HT_{1AR} antagonist and/or injection of the 5-HTergic neuronal neurotoxin 5,7-dihydroxytryptamine (5,7-DHT). This toxin is known to reduce the brain levels of 5-HT in both rats [36] and pigeons [37]. Moreover, 5,7-DHT decreases the density of binding sites to [^{3}H]8-OH-DPATin the brainstem of rats [38,39]. Additionally, behavioral studies have shown that this toxin is effective in discriminating between the functions of pre- and postsynaptic 5-HT_{1ARs} in rats [40,41] and pigeons [42]. In the present report, we first describe the distribution of [^{3}H]8-OH-DPAT-binding sites in the brainstem and the hypothalamus of pigeons, as well as that of neurons activated (c-Fos-immunoreactive) by ICV injection of DPAT in the brainstem and in periventricular diencephalic areas. Furthermore, the effects of pretreatment with 5,7-DHT or a 5-HT_{1AR} antagonist (MM77) that primarily acts at postsynaptic 5-HT_{1ARs} [43] on 5-HT- and DPAT-evoked behaviors were examined.

2. Materials and methods

All experimental procedures described here were conducted in adherence to the recommendations of the "Principles of Animal Care" (NIH, 1985) and were approved by the local Committees for Ethics in Animal Research (protocols: Federal University of Santa Catarina, 23080.0383262/2008-65; Ruhr Universität, 8.87-50.10.37). Adult domestic pigeons (*Columba livia* of both sexes, 400–500 g body weight) were supplied by the central vivarium facilities of each university and were maintained in individual cages at a temperature of 22–24 °C in a 12:12 light-dark cycle (lights on at 07:00 a.m.; fluorescent daylight lamps generating 80–90 lx light intensity) with free access to food and water until the experiments.

2.1. Lateral ventricle cannula implant and 5,7-DHT injection procedures

The pigeons received an injection of desipramine hydrochloride (25 mg/kg/1 ml in 0.9% NaCl, i.p.; Sigma–Aldrich Co., St. Louis, MO, USA) to preserve the noradrenergic circuits from the deleterious effects of the neurotoxin 5,7-DHT (5,7-dihydroxytryptamine creatinine sulfate salt, Sigma–Aldrich Co., St. Louis, MO, USA); 30 min later, they were anesthetized (ketamine: 0.15 ml/100 g, xylazine: 0.05 ml/100 g, i.m.) and placed in the stereotaxic apparatus (David Kopf Instruments, Tujunga, CA, USA). All wound margins and the external acoustic meati (into which the stereotaxic inner bar was inserted) were infiltrated with lidocaine solution (5%). The animals received bilateral ICV injections (at AP = +6 mm; L = 1.5 mm; H = −5 mm; the stereotaxic coordinates were derived from the stereotaxic atlas of the pigeon brain [44]) of 5,7-DHT (Lesion group, 200 μg/ventricle) or vehicle (Veh group) using a guide cannula (21 G). 5,7-DHT was dissolved in 10 μl of 0.1% ascorbic acid/0.9% NaCl solution 10 min prior to the injections. In the 5-HT- and DPAT-treated animals (see Section 2.10.3 for details), the guide cannula was inserted into the right lateral ventricle, fixed to the skull using dental cement and 2 jeweler's screws, and maintained patent using a removable inner stylet. The injections were performed using an inner cannula (30 G) extending 1 mm from the tip of the guide cannula; and the inner cannula was connected to a Hamilton microsyringe using polyethylene tubing (injection rate; 0.5 μl/min). After these surgeries, the animals were treated (daily for the next 5 days) with the antibiotic Baytril® (5% enrofloxacin, Bayer; 0.1 ml/kg, i.m.) and the analgesic Ketofen® (Ketoprofen1%; Merial; 0.2 ml/kg, i.m.). The wound was treated daily with Furacin® cream (Nitrofural; Mantecorp). A post-operation recovery period of at least 10 days was observed before the experiments.

2.2. Drugs and ICV injections

5-HT (5-hydroxytryptamine hydrochloride; Sigma–Aldrich, St. Louis, MO, USA; dose 150 nmol) and DPAT [8-hydroxy-2 (di-*n*-propylamino) tetralin; Sigma–Aldrich, St. Louis, MO, USA; dose 30 nmol], a 5-$HT_{1A/7}$ receptor agonist, were dissolved in 5% ascorbic acid in 0.9% NaCl solution (used as the vehicle), and MM77 [1-(2-methoxyphenyl)-4-(4-succinimid-obutyl) piperazinedihydrochloride; Tocris Bioscience, Bristol, UK; dose 23 or 69 nmol], a postsynaptic 5-HT_{1A} receptor antagonist, was dissolved in 0.3% DMSO (in 0.02 M phosphate buffer solution; PBS); this solution was used as the vehicle for the MM77 pre-treatment experiments. 5-HT and DPAT were used in a dose range previously shown to induce ingestive and sleep-waking responses in free-feeding pigeons [9,12,13], and the MM77 doses were based on the effective systemic dose (divided by 1000) used to block DPAT-induced anxiolytic effects in rats [45]. The ICV injections were performed using a Hamilton microsyringe as described above. The volume injected (2 μl) was administered over a period of 2 min, and for the subsequent 2 min, the inner cannula was maintained in the cannula guide to avoid potential reflux of the solution.

2.3. Immunohistochemistry

Unless otherwise stated, all washing and incubation steps during the following procedures were performed under gentle shaking at room temperature (RT). The washing steps consisted of three washes (5 min each) with 0.1 M PBS containing 0.25% Triton X-100 (PBST). To detect c-Fos protein expression, free-floating sections were washed, blocked for 40 min in 2% bovine serum albumin (BSA) in PBST and incubated in the anti-c-Fos primary antibody (1:2000; rabbit anti-c-Fos; K-25 – Sc-253 – Santa Cruz Biotechnology, Dallas, TX, USA) in PBST solution containing 1% BSA in a humidified chamber for 18 h at 4–8 °C. Next, the sections were washed, the endogenous peroxidase activity was blocked by incubation in 0.3% H_2O_2 in 100% methanol for 40 min, and the sections were incubated (in PBST at RT) in a goat anti-rabbit biotinylated secondary antibody (1:1000; Vector Laboratories, Burlingame, CA, USA). After 2 h of incubation, the sections were incubated in the avidin–biotin complex (1.5 h; 1:1000 in PBST, Vector Laboratories). After washing, c-Fos labeling was visualized using 0.05% 3,3-diaminobenzidine (DAB; Sigma–Aldrich, St. Louis, MO, USA), 0.05% nickel ammonium sulfate and 0.015% H_2O_2 in 0.1 M PBS for 4–5 min, staining the immunopositive nuclei as dark gray/black. To detect c-Fos expression in serotonergic neurons, brainstem sections were stained with an antibody against the enzyme tryptophan hydroxylase (TPH) as described in [12]. Free-floating sections were washed, blocked for 40 min with 2% normal rabbit serum (NRS) in PBST and incubated in the anti-TPH primary antibody (1:1000; sheep anti-TPH: AB 1541, Millipore Corporation, Billerica, MA, USA) in PBST containing 1% NRS in a humidified chamber for 18 h at 4–8 °C. Next, the sections were washed and incubated (2 h in PBST at RT) in a rabbit anti-sheep biotinylated secondary antibody (1:1000; Vector Laboratories), followed by incubation in the avidin-biotin complex (1.5 h; 1:250 in PBST). TPH labeling was visualized using 0.05% DAB and 0.0075% H_2O_2 in 0.1 M PBS for 9 min, resulting in reddish-brown staining. The reaction was stopped by washing for 5 min in cold (4 °C) distilled water, and the sections were mounted on chrome-alum-gelatin-coated glass slides, air-dried for 48 h, and dehydrated in a graded alcohol series and xylene, followed by coverslipping using DPX (Fluka BioChemika, Sigma–Aldrich, St. Louis, MO, USA).

2.4. Cell counting

The sections were analyzed under an optical microscope (Olympus, BH-2), and images were captured using an attached camera

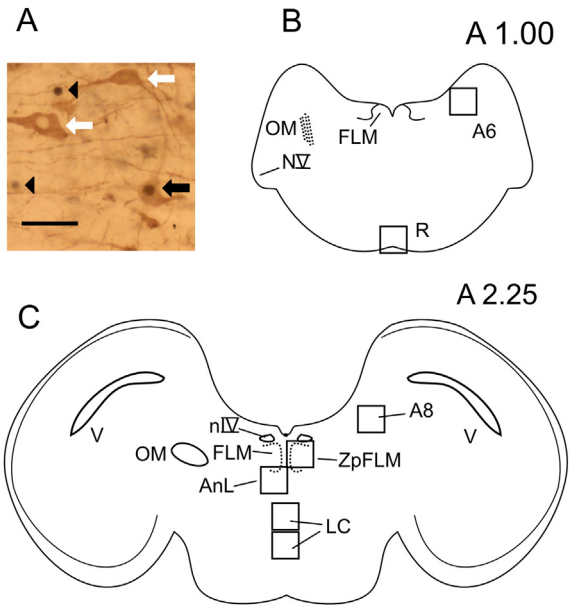

Fig. 1. (A) Photomicrograph illustrating c-Fos expression (black arrowhead) in a representative counted field indicating TPH-immunoreactive (TPH+, white arrow) and c-Fos− and TPH-immunoreactive cells (c-Fos+/TPH+, black arrow). Scale bar = 100 μm. (B) and (C) Schematic drawings of frontal sections of the pigeon brainstem showing the location of the quantified fields in the analyzed areas. The approximate rostrocaudal levels based on the Karten and Hodos' [44] atlas of the pigeon brain are indicated in the upper right corner of each drawing. For abbreviations, see the list.

(PixeLink, Ontario, Canada). The TPH- and c-Fos immunoreactive cells were analyzed according to our previous studies on the brainstem distribution of serotonergic neurons in pigeons [46,12], and the atlas of the pigeon brain of Karten and Hodos [44] was used to standardize the rostrocaudal levels (Figs. 1 and 2). To ensure that sections at the same rostrocaudal level were selected across the groups, the sections were selected based on their relative position to landmarks specific for each nucleus (see Figs. 1 and 2). Three representative sections of each nucleus from each animal in the experimental groups were selected for counting. For bilateral structures, such as n.A6 in the brainstem, or for hypothalamic nuclei, the counts in each hemisphere were averaged. The landmarks used for brainstem structures were detailed in a former report [12]. In short, c-Fos-labeled (c-Fos+), TPH-labeled (TPH+) or double-labeled (c-Fos+/TPH+) cells were quantified in six brainstem nuclei (Fig. 1), by a single blind-to-condition person (TSS) on 1–2 entire field photomicrographs with ImageJ software (www.rsbweb.nih.gov/ij/) of sections containing the nucleus raphe pontis (R; 1 quantification field (QF; 0.47 mm × 0.36 mm) in sections corresponding to the A 1.00 stereotaxic level of the pigeon brain atlas [44]), A6 (or caudal LoC; 1 QF were positioned between the ventrolateral border of the fasciculus longitudinalis medialis (flm), the BC and the floor of IV ventricle at the A 1.00 stereotaxic level), nucleus linearis caudalis (LC; 2 QF located over the 2 midline cell rows of the LC, at A 2.25 stereotaxic level), A8 (rostral part of the LoC; 1 QF were aligned vertically to the TIO and horizontally aligned to the flm at the A 2.25 stereotaxic level), nucleus annularis (Anl, 1 QF positioned immediately ventral to the flm along its mediolateral extent and dorsally to the DBC fibers, at the A 2.25 stereotaxic level) and the zone perifasciculus longitudinalis medialis (Zp-flm; 1 QF placed laterally to the IV ventricle, and medially to the flm and ventral to the nIV (Fig. 1) dorsomedial to the flm and lateral to the 4th IV ventricle, and 2 fields were placed laterally to the flm) (Fig. 3).

The identification and nomenclature of hypothalamic areas and other prosencephalic structures were based on the reviews by Kuenzel and Van Tienhoven [47] and Reiner and cols [48]. Counting of c-Fos labeling in these regions and landmarks used to locate the diencephalic QFs are described as following. The paraventricular organ (PVO; 1 QF positioned at a particular spot in periventricular region of the recessus infundibuli characterized by the presence of juxtaposed cells aligned in a bended way into the ventricular wall) and nucleus infundibuli (IN; 1 QF centrally positioned in the infundibulus region) were evaluated at the A 4.75 stereotaxic level [44], with the IF as landmark (Fig. 2). The nucleus paraventricularis (PVN; 2 QFs vertically aligned at paraventricular region of the dorsal hypothalamus); the nucleus dorsomedialis hypothalami (DMN; 1 QF, dorsally); the nucleus ventromedialis hypothalami (VMN; 1 QF, medioventrally) and the lateral hypothalamic area (LHy; 1 QF, laterally located) were analyzed at the A 6.75 stereotaxic level [44], where the DSD and DSV are very visible in the ventral part of hypothalamus (Fig. 2). The bed nucleus of stria terminalis, pars lateral (BSTNl; 1 QF, ventrolateraly located to the lateral ventricle); the septal lateral nucleus (SL; 1 QF, ventromedialy located to lateral ventricle) and the subfornical organ (SFO; 1 QF, located at the "roof" of the III ventricle, posterior to the CA) were evaluated in the A 7.25 stereotaxic level [44], where OM's ascending fibers are visible. To evaluation of the nucleus preopticus medialis (POM), 2 QFs were vertically arranged on this nucleus ventrally to the CA (at A 7.75 stereotaxic level [44]), and to the nucleus preopticus anterior (POA), 1 QF was positioned on its entire area, with the TSM dorsolaterally located as reference (stereotaxic level A 9.25 [44]) (Fig. 2).

2.5. Behavioral analysis

During the first hour after the second injection (see the experimental protocols below), video recordings (Orbit QuickCam, V-UCC22, Logitech, Newark, CA, USA) of the home cage were captured. The latency to the first event, the total duration and frequency of drinking, feeding, preening, locomotor, exploratory, alert immobility and sleep-like behavior (SLB) were scored using the behavioral analysis software EthoWatcher® ([49]; freely available at www.ethowatcher.ufsc.br). The behavioral events have been described previously (e.g., [12,13]) and are shown in a movie clip that is available online [50]. Food pellets were delivered via plastic cups, and water was provided in plastic bottles. The experiments were performed between 10:00 and 16:00 h during the illuminated period of the light/dark cycle, when the ingestive behavior of pigeons is stable and low [12]. Food and water were weighed 1 h after the final injection.

2.6. Receptor autoradiography

The 5-HT-binding sites of the 5-HT_{1AR} were labeled with [^{3}H] 8-OH-DPAT [51,52] according to a previously published standardized protocol [53,54,33], which consisted of three steps. (1) The samples were preincubated for 30 min (at RT) in buffer (170 mM Tris–HCl buffer containing 4 mM $CaCl_2$ and 0.01% ascorbic acid, pH 7.6) to remove endogenous ligands from the tissue; (2) The 5-HT binding sites were labeled via incubation in 1 nM [^{3}H]8-OH-DPAT in buffer for 60 min at room temperature in the presence or absence of 1 μM 5-hydroxytryptamine as a displacer (non-specific binding or total binding, respectively). Specific binding was calculated as the difference between total and non-specific binding. Because non-specific binding accounted for less than 10% of total binding, total binding was considered to be equivalent to specific binding. (3) The samples were rinsed for 5 min at 4 °C in buffer to eliminate the unbound radioactive ligand from the sections. The sections were air-dried overnight and subsequently co-exposed for 8 weeks to a tritium-sensitive film (Hyperfilm, Amersham, Braunschweig, Germany) and plastic [^{3}H]-standards (Microscales, Amersham) of

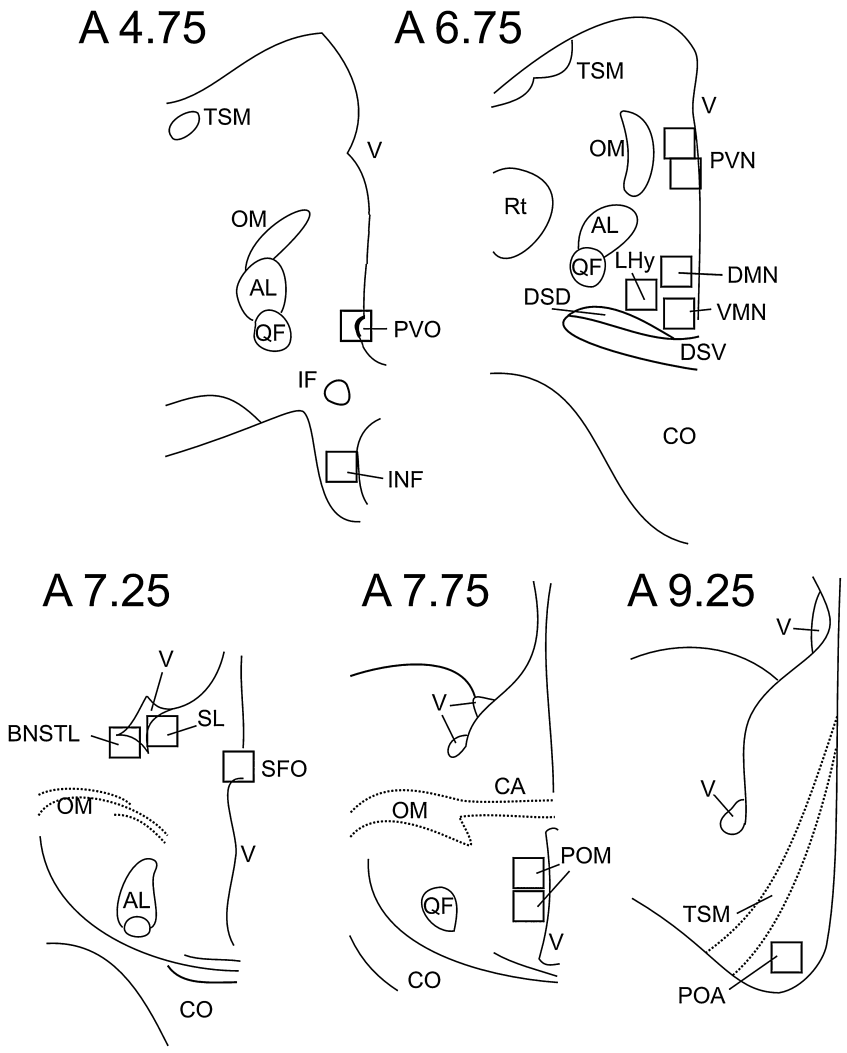

Fig. 2. Schematic drawings of frontal sections of the pigeon brain showing the hypothalamic and subpallial structures (SL and BNSTl) and the location of the quantified fields in the analyzed areas. The approximate rostrocaudal levels based on Karten and Hodos' [44] atlas of the pigeon brain are indicated in the upper right corner of each drawing. For abbreviations, see the list.

known levels of radioactivity. Adjacent sections were Nissl stained for cytoarchitectonic analysis.

2.7. Image analysis and anatomical identification

Autoradiographs were digitized [55,53] using a KS-400 image analysis system (Kontron, Germany) connected to a CCD camera (Sony, Tokyo) equipped with an S-Orthoplanar60-mm macro lens (Zeiss, Germany). The images were collected at a resolution of 512×512 pixels and 8-bit gray value. Images of the co-exposed microscales were used to compute a calibration curve via nonlinear, least-squares fitting, which defined the relationship between the gray values in the autoradiographs and the levels of radioactivity. This calculation enabled the pixel-wise conversion of the gray values of an autoradiograph to the corresponding levels of radioactivity. These concentrations of the binding sites occupied by the incubated ligand were transformed into receptor binding site densities under saturation conditions according to the function $(K_d + L)/A_s \times L$, where K_d is the equilibrium dissociation constant of ligand-binding, L is the concentration of the incubated ligand, and A_s is the specific activity of the ligand. The borders of the structures as defined by the atlas of Karten and Hodos [44] were microscopically identified in the sections processed for the visualization of cell bodies and were traced on prints of the digitized autoradiographs. For the identification of anteroposterior levels of the different structures, we used the same landmarks as those used to cell counting (Section 2.5; Figs. 1 and 2). The DMN and PVN nucleus, through autoradiographs process, were separated into PMH and PLH (the DMN) and into pars magnocellularis (PVNm) and pars parvocellularis (PVNp) (the PVN). The mean of the gray values of the anatomically identified brain regions (from one to five sections per animal and region) were transformed into the binding site concentration (fmol/mg protein).

2.8. High pressure liquid chromatography (HPLC)

2.8.1. Drugs and reagents

Standards of 5-HT, 5-hydroxyindoleacetic acid (5-HIAA), noradrenaline (NA), their metabolites 5-hydroxyindoleacetic acid (5-HIAA) and homovalenic acid (HVA), and all salts for mobile-phase extraction were acquired from Sigma–Aldrich (St. Louis, MO, USA). HPLC grade solvents (J.T. Baker, Mexico) and Milli-Q water (Millipore, São Paulo, Brazil) were used without further purification.

2.8.2. HPLC apparatus

HPLC was performed using a Waters e2695 Alliance Separation Module composed of a quaternary pump, a degasser, a column

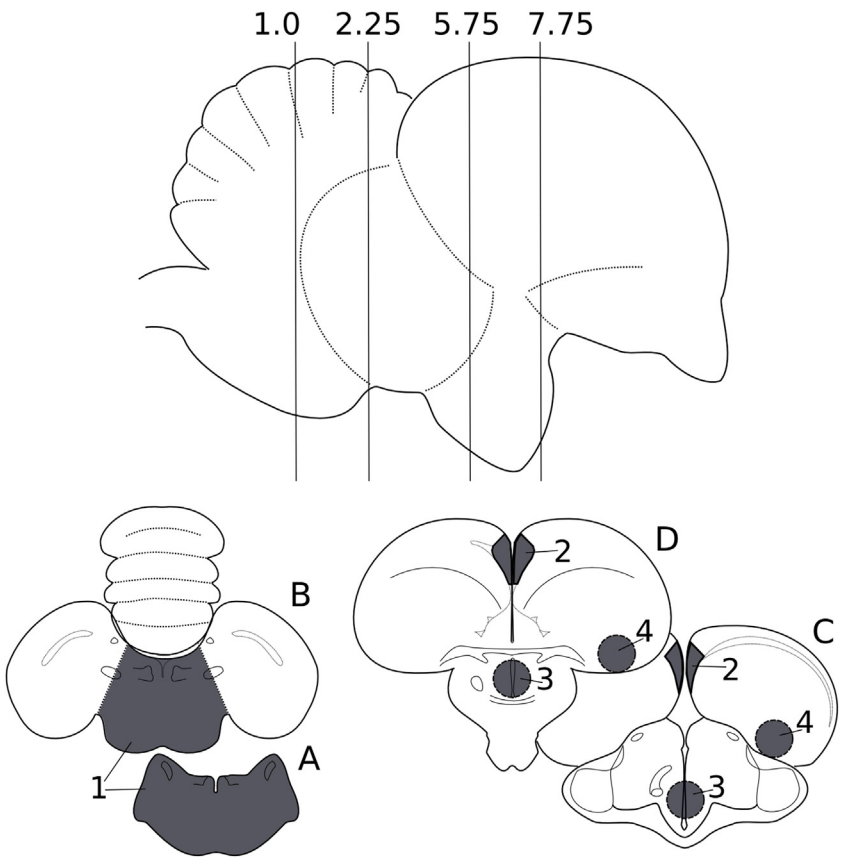

Fig. 3. Upper panel: sagittal view of the pigeon brain showing the anterior-posterior levels at which different sections were evaluated. Lower panels: schematic drawings of the frontal sections of the pigeon brain showing the dissected structures (dark area) at which the levels of 5-HT were measured. The numbers indicate the following structures: 1 – brainstem; 2 – hippocampus; 3 – hypothalamus; and 4 – arcopallium. The letters A–D correspond to the specific antero-posterior levels indicated in upper panel: (A) A1.0; (B) A2.25; (C) A5.75; and (D) A7.75. These coordinates are derived from the atlas of the pigeon brain of Karten and Hodos [44].

heater and a refrigerated autosampler (maintained at 4 °C) coupled to a Waters 2465 amperometric electrochemical detector. The chromatograms were acquired and processed using Empower® 2 software (Waters, Milford, MA, USA).

2.8.3. Chromatographic conditions

The chromatographic analysis was adapted from Linder and cols. [56]. The mobile phase mixture was prepared as 90 mM sodium dihydrogen phosphate, 50 mM citric acid, 50 μM disodium EDTA, 1.7 mM sodium 1-heptanesulfonate:acetonitrileat 90:10, which was adjusted to pH 3.0 using concentrated NaOH, filtered using a 0.45 μm cellulose acetate membrane (Merck Millipore, Billerica, MA, USA), and degassed under vacuum in an ultrasonic bath prior to use. The mobile phase was pumped in an isocratic mode at a flow rate of 0.30 ml/min through a reverse-phase (C18) semi-μHPLC column (150 mm length × 2 mm inner diameter, 4 μm diameter particle size; Synergi Hydro RP, Phenomenex, Torrance, CA, USA), protected with a C18 guard-column (20 mm length × 2 mm inner diameter; Alltech, Deerfield, IL USA), both maintained at 35 °C. The electrochemical reactions occurred in an electrochemical flow cell equipped with a glassy carbon working electrode (GC-WE) operated in direct current (DC) mode set at an oxidation potential of +400 mV vs. an "In Situ Ag/AgCl" (ISAAC) reference electrode and a stainless steel wire auxiliary electrode (Waters, part # 205004215). The peaks of the analytes were identified via comparison of the retention times to the respective standards. The peak areas were integrated to quantify the samples via linear regression of the standard calibration curve. The values obtained were expressed as ng/mg wet tissue.

2.8.4. Sample preparation for HPLC analysis

The sample preparation protocol was adapted from Alesci and Bagnoli [37]. To section the brain of different pigeons at similar predetermined levels (Fig. 1), we developed an acrylic matrix adapted for the pigeon brain (similar to a rodent brain slicer, commercially available) based on the atlas of the pigeon brain by Karten and Hodos [44]. Briefly, the brain tissues (brainstem, hypothalamus, hippocampus, and arcopallium; Fig. 1) were removed from the skull on ice and stored in Eppendorf tubes containing 0.3 ml of refrigerated buffer (0.1 M perchloric acid + 0.02% sodium meta-bisulfide) and immediately stored at −80 °C until analysis. The tissue samples were crushed manually and sonicated in an ultrasonic cooling bath for 10 min. Then, the Eppendorf tubes were promptly centrifuged (14,000 rpm) at 4 °C for 20 min, and 20 μl of the supernatant was injected into the HPLC column.

2.9. Statistical analysis

The behavioral, food and water intake data were analyzed via 2-way ANOVA (factors: pretreatment × treatment, experiment 2.9.2; lesion × treatment, experiment 2.9.3) followed by Scheffé post hoc analysis for any significant results. The cell labeling density (number of cells per mm^2) was analyzed separately for each brain area in each experimental group (experiments 2.9.4 and 2.9.5). First, the counting data were analyzed using Shapiro–Wilk's test to verify the normality of the particular data sample. Then, the data were analyzed via a parametric (one way ANOVA) or non-parametric (Kruskal–Wallis test) analysis, followed by respective post hoc analysis (parametric: Sheffé post hoc analysis; non-parametric: Mann–Whitney *U* test) when appropriate. For experiment 2.9.3, the

alterations in the 5-HT levels (expressed as the % of the 5-HT levels in the control animals) were analyzed using the non-parametric Kruskal–Wallis test followed by the Mann–Whitney *U* post hoc test to evaluate the inter-group differences. To demonstrate the [^{3}H]-8-OH-DPAT-binding sites in the brainstem and the hypothalamus, we performed descriptive analysis of the data expressed as the means and standard deviation (SD). All analyses were performed using Statistica 8.0 software (Stasoft, Tulsa, OK, USA). For all tests, p values of <0.05 were considered to be statistically significant.

2.10. Experimental procedures

2.10.1. Distribution of 5-HT$_{1AR}$ binding sites in the brainstem and the hypothalamus of the pigeon brain

The animals (N = 6 pigeons, of both sexes) were deeply anesthetized with equithesin (i.m.; 0.5 ml/kg bw), decapitated and their brains were removed from the skull, frozen immediately in isopentane at −40 °C and stored at 70 °C. Serial coronal 10 μm sections were generated using a cryostat microtome (2800 Frigocut E, Reichert-Jung, Vienna, Austria). The sections were thaw-mounted on gelatinized slides and freeze-dried before use for receptor autoradiography or histological staining to visualize cell bodies [57].

2.10.2. Effects of pretreatment with MM77 on the ingestive and behavioral responses evoked by ICV injection of 5-HT or DPAT

Sixteen experimentally naïve pigeons were cannulated ICV (see procedures in the Section 2.1) and were separated into two groups: (1) 5-HT group: 8 animals treated with vehicle and 5-HT (150 nmol) (7 days interval between the treatments) and (2) DPAT group: 8 animals treated with vehicle and DPAT (30 nmol) (7 days interval between injections). In both groups, the injections (5-HT; DPAT or vehicle) were preceded (20 min) with an injection of MM77 or vehicle. For the 5-HT-injected animals, we tested two different doses of MM77: 23 and 69 nmol; for the DPAT animals, we tested only the most effective MM77 dose, 69 nmol (based on a previous finding of the most evident 5-HT-mediated effect, a dipsogenic response). Each pigeon received all treatments corresponding to its specific experimental group, which was assigned according to a Latin-squared design. In the end, each group was formed by the following treatments: 5-HT group: veh × veh; veh × 5-HT; MM77 (23) × veh; MM77 (69) × veh; MM77 (23) × 5-HT; MM77 (69) × 5-HT; DPAT group: veh × DPAT; MM77 (69) × DPAT. As to 5-HT and DPAT we used the same vehicle (ascorbic acid), we did not repeated the treatments veh × veh and MM77 × veh in the DPAT group.

2.10.3. Effects of the neurotoxin 5,7-DHT on the ingestive and behavioral responses evoked by 5-HT and DPAT and on the density of brainstem serotonergic neurons

Twenty-four animals were cannulated ICV billateraly (see procedures in the Section 2.1) and divided into 2 groups: (1) 12 animals (6 injected with 5,7-DHT and 6 sham-injected), sacrificed 12 days after the lesion (group DHT12) and (2) 12 animals (6 injected with 5,7-DHT and 6 sham-injected), sacrificed 28 days after the lesion (group DHT28). The animals from group DHT12 were used to verify the effects of 5,7-DHT on the 5-HT levels at the 12th day after 5,7-DHT treatment. The animals from group DHT28 were subjected to pharmacological experiments (from day 12–27) to evaluate the effects of 5,7-DHT on the ingestive and behavioral responses produced by 5-HT and DPAT (according to protocols similar to those described above). Each animal in the group DHT28 were evaluated using all drugs (7-day interval between treatments). On 12th or 28th day, the animals were sacrificed via anesthetic overdose (50 mg/kg ketamine hydrochloride and 10 mg/kg xylazine, IM) and decapitated. Then, the brains were quickly removed from the skull and immediately stored at −80 °C until analysis. To examine the effects of 5,7-DHT on the density of brainstem serotonergic neurons, we used another 12 naïve pigeons (6 treated with 5,7-DHT and 6 sham-injected). These animals were anesthetized (50 mg/kg ketamine hydrochloride and 10 mg/kg xylazine, IM) and perfused (see details in Section 2.10.4) 12 days after the injection, and their brains were prepared for immunohistochemistry to verify the effects of 5,7-DHT on the number of TPH-immunoreactive cells.

2.10.4. Effects of DPAT ICV injection on c-Fos expression in TPH-immunoreactive and -non-immunoreactive neurons in serotonergic brainstem areas

In a previous study [12], we described the effects of ICV injection of 5-HT into free-feeding pigeons on c-Fos activation in serotonergic (TPH+) and non-serotonergic (c-Fos+/TPH−) cells in the brainstem. DPAT and 5-HT exert similar effects on drinking and sleep [13]. Here, we examined the effects of ICV injection of DPAT on the pattern of c-Fos expression in TPH-immunoreactive and non-immunoreactive cells. Moreover, as we noted previously [12], water intake after these injections produced a different pattern of c-Fos expression. Therefore, we used the same experimental design to test the effects of 5-HT [12]. Fifteen pigeons (both sex, 480–540 g) were cannulated ICV (see procedures in the Section 2.1), assigned to one of three groups (N:5/group) and injected ICV as follows: (1) vehicle (5% ascorbic acid in 0.9% NaCl solution; vehicle group), (2) DPAT (30 nmol) with free access to water after the injection (DPAT + W group) or (3) DPAT (30 nmol) with no access to water (DPAT group). The vehicle-treated animals were provided with free access to water. The behaviors of the animals were recorded for the first 90 min after injection, and water/food intake was quantified at the end of this period. Then, the animals were deeply anesthetized (50 mg/kg ketamine hydrochloride and 10 mg/kg xylazine, IM) and were transcardially perfused with heparin (IVC bolus of 1500 IU) and a sucrose solution (9.25% in 0.02 M phosphate buffer (PB), pH 7.2, at 37 °C) followed by 4% paraformaldehyde in PB. The brains were removed, blocked, post-fixed for 4 h in the same fixative, sectioned at 40 μm using a vibratome (Vibratome 1500 Plus, Vibratome Company, St. Louis, MO, USA) and stored in a cryoprotectant solution at −20 °C until use.

2.10.5. Effects of DPAT and 5-HT ICV injection on c-Fos activation in the hypothalamus and in the prosencephalic periventricular areas

A group of 10 ICV-cannulated, experimentally naive pigeons, which were maintained as described above, were separated into two groups and treated as follows: (1) 5-HT (150 nmol) ICV injection with free access to water (5-HT + W group) and (2) 5-HT ICV injection with no access to water (5-HT group). The experimental procedures, including perfusion and brain preparation, were the same as those described in Section 2.10.4. The data from these groups were compared to the vehicle group described in Section 2.10.4. In Figs. 9 and 10 and in Table 3, the DPAT (N:5) and 5-HT groups (N:5) were only compared to the control group (N:5).

3. Results

3.1. Distribution of 5-HT$_{1AR}$ binding sites in the brainstem and the hypothalamus of the pigeon brain

In both the brainstem and the hypothalamus, [^{3}H]8-OH-DPAT binding sites were most apparent in structures located at the midline or in periventricular (third ventricle) and periaqueductal regions (Table 1; Fig. 4). [^{3}H]8-OH-DPAT binding was intense in the dorsal region of the pons, concentrated in the peri-fasciculus longitudinalis medialis zone (ZpFLM; Fig. 4A; Table 1), in area A6 (the caudal portion of the locus coeruleus; Fig. 4A, Table 1), and in the caudal portion of the griseum centralis (GCt; Fig. 4A; Table 1).

Table 1
[^{3}H]8-OH-DPAT binding values (fmol/mg protein) in brainstem and hypothalamus of the pigeon (N = 6 animals). Data is presented as mean ± SD. The percentage binding values for each structure and the qualitative classification are compared to structure with the maximal binding value (MBV). Brainstem and hypothalamic nuclei are presented in a caudorostral arrangement. ++++, very high; +++, high; ++, moderate; + low.

Brain area	Binding density			
	fmol/mg protein	±SD	Relative density compared with MBV (%)	
Brainstem				
R (nucleus raphe pontis)	180	133	34	++
LoC caudalis (A6)	351	238	68	+++
LoC rostralis (A8)	41	19	8	+
SCd (N. Subcoeruleus dorsalis)	46	19	9	+
SCv (N. Subcoeruleus ventralis)	33	15	6	+
LC (N. Linearis caudalis)	345	161	66	+++
CS (N. Centralis Superior)	138	144	26	++
ZpFLM (Zone Peri Fasciculus Longitudinalis Medialis)	510	289	98	++++
Anl (N. Annularis)	517	222	100	MBV ++++
GCt caudalis (Substantia Gricea Centralis, pars caudalis)	315	166	61	+++
GCt rostralis (Substantia Gricea Centralis, pars rostralis)	38	13	7	+
PME (Posterior median eminence)	144	71	27	++
RPO (N. Reticularis Pontis Oralis)	24	15	5	+
Hypothalamus				
IN (N. Infundibuli Hypothalami)	57	44	11	+
PVO (Organum Pavaventriculare)	444	179	86	+++
MM (N. Mamillaris Medialis)	250	137	48	++
ML (N. Mamillaris Lateralis)	36	13	7	+
PMM (N. Premamillaris)	179	64	34	++
VMN (N. Ventromedialis Hypothalami)	102	24	20	+
LHy (N. Lateralis Hypothalami)	98	29	19	+
SCI (Stratum Cellulare Internum)	31	26	6	+
SCE (Stratum Cellulare Externum)	25	3	5	+
PVNm (N. Paraventricularis, pars magnocellularis)	171	35	33	++
PVNp (N. Paraventricularis, pars parvocellularis)	82	51	16	+
PLH (N. Lateralis Hypothalami Posterioris)	112	72	22	++
PMH (N. Medialis Hypothalami Posterioris)	229	164	44	++
AM (N. Anterior Medialis Hypothalami)	48	61	9	+
POM (N. Preopticus Medialis)	103	35	20	+
POA (N. Preopticus Anterior)	357	115	69	+++
PPM (N. Magnocellularis Preopticus)	143	77	27	++
FDB (Fasciculus Diagonalis Brocae)	273	133	53	+++
SOe (N. Supraopticus externus)	258	85	50	++
PD (N. Preopticus Dorsalis)	274	90	53	+++

Discrete labeling was detected in the rostral portion of the GCt (Fig. 4B; Table 1). Moderate labeling was detected in the midline ventral raphe nucleus (Fig. 4A; Table 1). In the mesencephalon, the highest densities of [^{3}H]8-OH-DPAT labeling were detected in the medial portion of the nucleus annularis (Anl) and in the rostral portion of ZpFLM (Fig. 4B; Table 1). The Anl displayed the maximal binding value (MBV; 517 fmol/mg protein = 100%), to which all other structures were compared. In the pontomesencephalic midline, the linearis caudalis (LC) and centralis superior (CS) nuclei displayed high and moderate levels of [^{3}H]8-OH-DPAT binding, respectively (Fig. 4B; Table 1). Modest labeling was observed in the lateral monoamine-containing nuclei sub coeruleus dorsalis (SCd) and in the sub coeruleus ventralis (SCv) (Table 1), in area A8 (the rostral portion of the locus coeruleus; Fig. 4B; Table 1), and in the reticularis pontis oralis nucleus (RPO) (Table 1).

Binding to [^{3}H]8-OH-DPAT in the hypothalamus and the preoptic region was highly localized to medial structures. In the posterior hypothalamus, the highest concentration of all hypothalamic nuclei investigated was detected in the paraventricular organ (PVO; 86% of the staining in the MBV, the Anl; Fig. 4D; Table 1), a bilateral circumventricular organ that is located at the posteroventral wall of the third ventricle. The posterior median eminence (PME; another circumventricular organ), displayed moderate expression of [^{3}H]8-OH-DPAT-binding sites (Fig. 4C; Table 1). We also found moderate labeling abutting the mamillaris medialis nucleus (MM; Fig. 4D; Table 1) and in the pre-mamillaris nucleus (PMM; Table 1). Discrete labeling was detected in the nuclei infundibuli (IN; Fig. 4D; Table 1) and in the mamillar lateralis (ML) (Table 1). In the medial hypothalamus, we detected moderate [^{3}H]8-OH-DPAT binding in the paraventricular nucleus (magnocellular portion, PVNm; 171 ± 35 fmol/mg protein; parvocellular portion, PVNp; 82 ± 51 fmol/mg protein; Fig. 4E; Table 1), in the nucleus preopticus medialis (POM) (Table 1), in the nucleus medialis hypothalami posterioris (PMH) and in the nucleus lateralis hypothalami posterioris (PLH, Fig. 4E; Table 1). Low levels of [^{3}H]8-OH-DPAT binding were detected in the nucleus lateralis hypothalami (LHy) (Fig. 4E; Table 1), in the stratum cellular internum (SCI), in the stratum cellulare externum (SCE) (Table 1) and in the anterior medialis hypothalami (AM) (Fig. 4E; Table 1). In the anterior hypothalamic and preoptic areas, medial (preopticus anterior, POA; magnocellularis preopticus, PPM; and preopticus dorsalis, PD) and lateral structures (supraopticus externus, SOe; fasciculus diagonalis Brocae, FDB) displayed moderate (PPM and SOe) to high (POA, PD and FDB; Fig. 4E; Table 1) levels of [^{3}H]8-OH-DPAT binding.

3.2. *Effects of pretreatment with MM77 on the ingestive and behavioral responses induced by ICV injection of 5-HT or DPAT*

Two-way ANOVA revealed that 5-HT injection produced significant changes in drinking behavior and SLB. 5-HT injection increased water intake ($F_{1,42}$ = 149, p = 0.001; interaction: $F_{1,42}$ = 9.2, p = 0.0004) (Fig. 5) and drinking frequency ($F_{1,42}$ = 149, p < 0.0001) and duration ($F_{1,42}$ = 32, p < 0.0001) and also decreased the latency to the first episode of drinking ($F_{1,42}$ = 7.5, p = 0.008; Table 1, Supplementary material). 5-HT also increased the SLB duration ($F_{1,42}$ = 12,

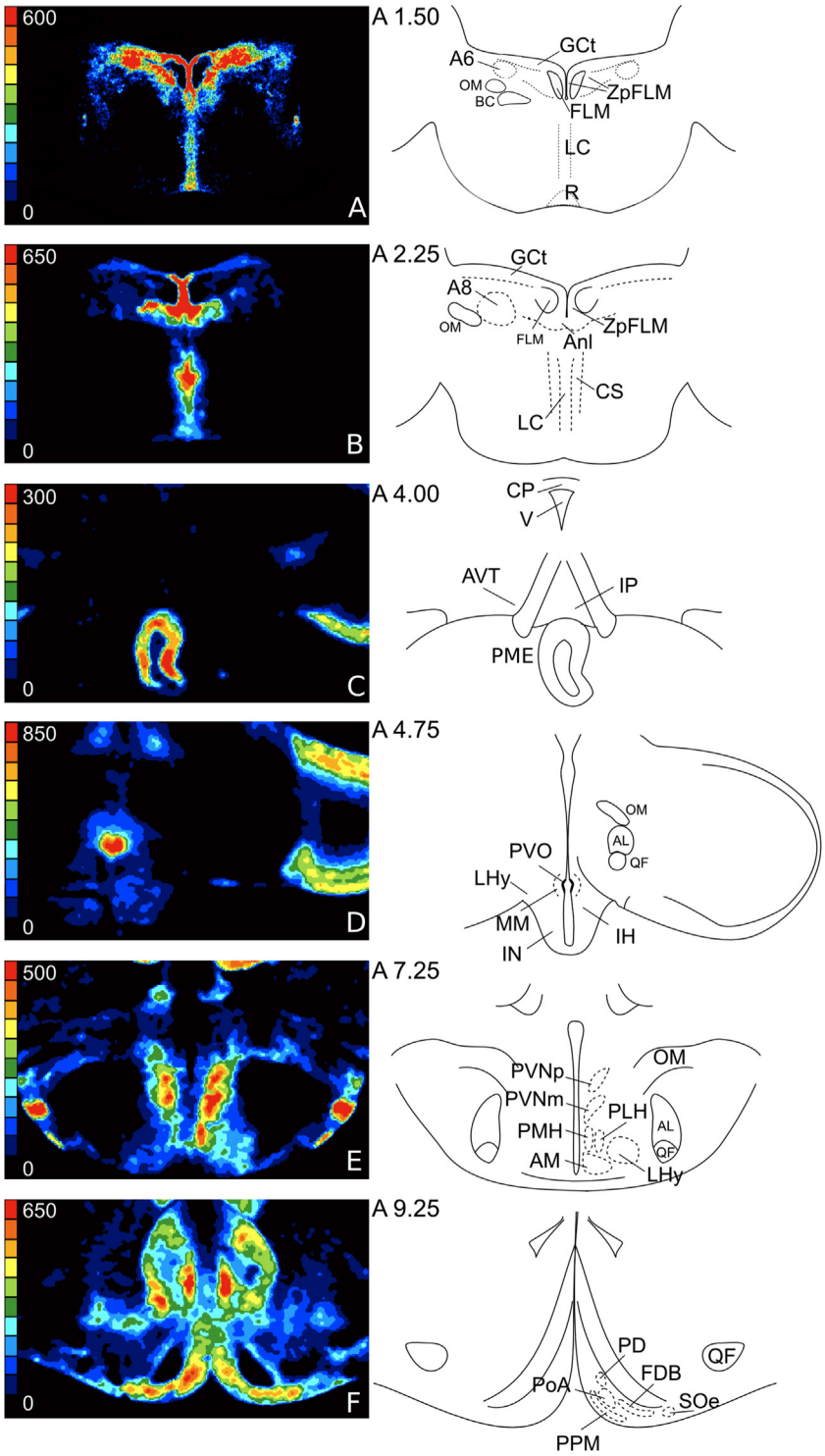

Fig. 4. Color-coded autoradiographs of [^{3}H]8-OH-DPAT binding in the pigeon brainstem (left column, A and B, letters in the lower right corner) and hypothalamus (C–F), arranged in caudo-rostral order. ($N = 6$ animals). The color-coding indicates the density of [^{3}H]8-OH-DPAT-binding sites in terms of fmol/mg protein. Note that the color-coding of each image is optimized to the overall DPAT-binding site density. The maximum DPAT binding level was detected in the AnI (Panel B). In the right column, schematic drawings of frontal sections of the pigeon brain show the structures examined. Alphanumeric characters placed at the upper left corner indicate the approximate stereotaxic levels according to the Karten and Hodos atlas [44]. For abbreviations, see the list and Table 1.

$p = 0.0004$; interaction: $F_{2,42} = 3.6$, $p = 0.0004$) (Fig. 5) and frequency (5-HT: $F_{1,42} = 6.2$, $p = 0.01$; interaction: $F_{2,42} = 3.2$, $p = 0.05$) and decreased the latency to the first SLB episode ($F_{1,42} = 6.1$, $p = 0.02$; interaction: $F_{2,42} = 3.2$, $p = 0.05$; Table 1, Supplementary material). However, 5-HT injection did not alter food intake or feeding behavior (Fig. 5). Pretreatment with MM77 reduced the effects of 5-HT on water intake (Fig. 5) and drinking duration (Table 1, Supplementary material). The MM77 23 nmol dose decreased the effect of 5-HT on drinking latency, and the 69 nmol dose blocked the effect of 5-HT on drinking frequency (Table 1, supplementary material). MM77 failed to alter food or water intake or feeding or drinking behavior (Fig. 5). Both MM77 doses completely blocked

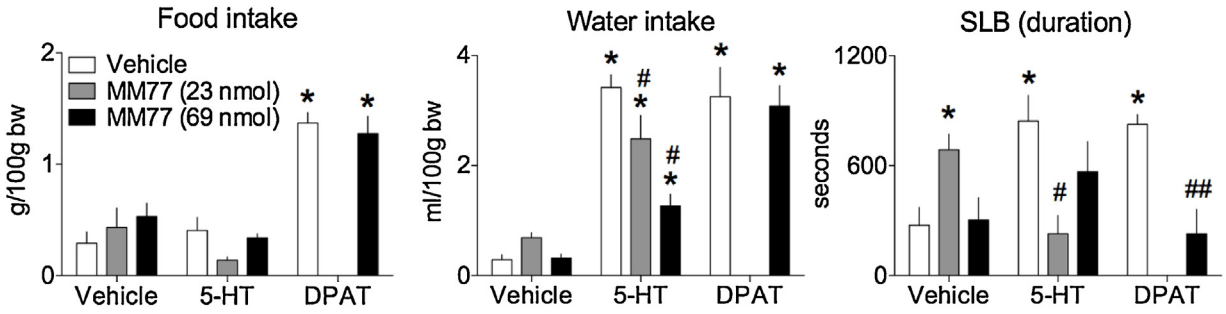

Fig. 5. The effects of ICV injection of 5-HT (0 or 150 nmol, $N = 8$) or DPAT (0 or 30 nmol, $N = 8$) on food and water intake and on sleep-like behavior (SLB duration after pretreatment with MM77 (0, 23 or 69 nmol)). The data are expressed as the means ± standard error of the mean (S.E.M.). $^{*}p < 0.05$ compared to animals treated with vehicle followed by vehicle injection; $^{\#}p < 0.05$ compared to animals treated with vehicle followed by 5-HT injection; and $^{\#\#}p < 0.05$ compared to animals treated with vehicle followed by DPAT injection.

the 5-HT-induced increase in the duration and latency of SLB (Fig. 5).

Supplementary Table S1 related to this article can be found, in the online version, at http://dx.doi.org/10.1016/j.bbr.2015.03.059.

Similarly, DPAT affected drinking behavior and SLB. Moreover, this treatment produced significant effects on feeding. DPAT injection increased water intake ($F_{1,20} = 40$, $p < 0.0001$) (Fig. 5) and drinking duration ($F_{1,20} = 34$, $p < 0.0001$) and frequency ($F_{1,20} = 7$, $p = 0.01$), and decreased the latency to the first drinking episode ($F_{1,20} = 14$, $p < 0.0001$) (Table 2, Supplementary material). DPAT injection increased food intake ($F_{1,20} = 43$, $p < 0.0001$) (Fig. 5) and feeding frequency ($F_{1,20} = 6.7$, $p = 0.01$) and duration ($F_{1,20} = 63$, $p < 0.0001$) and decreased the latency to the first episode of feeding ($F_{1,20} = 20$, $p = 0.0002$) (Table 2, Supplementary material). DPAT also increased the SLB duration ($F_{1,20} = 8.6$, $p = 0.008$; interaction: $F_{1,20} = 8.5$, $p = 0.008$) (Fig. 5) and decreased the latency to the first SLB episode ($F_{1,20} = 5.6$, $p < 0.0001$) (Table 2, Supplementary material). MM77 did not affect feeding or drinking behavior induced by DPAT. However, MM77 effectively blocked the effects of DPAT on SLB duration ($F_{1,20} = 8.5$, $p = 0.008$) (Fig. 5) and latency ($F_{1,20} = 6.6$, $p = 0.008$) (Table 2, supplementary material). The only per se effect of MM77 injection was a significant increase in SLB duration at the 23 nmol dose (Fig. 5).

Supplementary Table S2 related to this article can be found, in the online version, at http://dx.doi.org/10.1016/j.bbr.2015.03.059.

3.3. Effects of the neurotoxin 5,7-DHT on the ingestive and behavioral responses induced by ICV injection of 5-HT or DPAT

5,7-DHT injection reduced the 5-HT levels in the brainstem ($H_{4,29} = 17.2$, $p = 0.0017$), the hypothalamus ($H_{4,29} = 14.6$, $p = 0.005$) and the hippocampus ($H_{4,29} = 11.8$, $p = 0.01$) compared to the controls. However, 5,7-DHT did not alter the 5-HT levels in the arcopallium (Table 2). The analyses revealed no significant alteration in the 5-HT,NA or HVA levels in sham-injected compared to control pigeons. In the brainstem, a 56 ± 10% reduction in group DHT12 ($p = 0.02$) and a 65 ± 7% reduction in group DHT28 ($p = 0.013$) were detected (Table 2) compared to the corresponding vehicle-treated groups. In the hypothalamus, this reduction was of 80 ± 33% ($p = 0.003$) in group DHT12 and 70 ± 22% in group DHT28 ($p = 0.012$; Table 2). In the hippocampus, we detected 66 ± 35% and 40 ± 20% reductions in the DHT12 and DHT28 groups, respectively (Table 2). 5,7-DHT injection also decreased the level of the 5-HT metabolite 5-HIAA in the hypothalamus ($H_{4,29} = 10$, $p = 0.01$) and in the hippocampus ($H_{4,29} = 7.4$, $p = 0.001$) in both the DHT12 and DHT28 groups. We did not detect any significant change in the 5-HIAA levels in the brainstem or the arcopallium in any group injected with 5,7-DHT (data not shown). Moreover, 5,7-DHT did not affect the NA or HVA levels in any examined structure (data not shown). Furthermore, injection of 5,7-DHT decreased the number of TPH+ neurons in the brainstem. This effect of 5,7-DHT was detected in all serotonergic areas, and the most affected nuclei are depicted in Fig. 6. Two-way ANOVA revealed that 5-HT and DPAT increased water intake ($F_{2,24} = 88$, $p < 0.0001$) and SLB ($F_{2,24} = 20$, $p < 0.0001$). Moreover, DPAT increased food intake ($F_{2,24} = 53$, $p < 0.0001$) (Fig. 7). Injection of 5,7-DHT did not affect the ingestive or hypnogenic effect of 5-HT or DPAT. Additionally, 5,7-DHT increased SLB induced by 5HT but did not affect SLB or feeding stimulated by DPAT (Fig. 7).

3.4. Effects of DPAT ICV injection on c-Fos activation in TPH-immunoreactive and -non-immunoreactive neurons in serotonergic brainstem areas

Injection of DPAT increased the number of c-Fos-immunoreactive (c-Fos+) cells in Anl ($H_{2,15} = 10$, $p = 0.006$) and ZpFLM ($H_{2,15} = 13$, $p = 0.001$) (Fig. 8). Moreover, DPAT increased the number of double-labeled (c-Fos+/TPH+) cells in the LC ($H_{2,15} = 9.8$, $p = 0.007$), Anl ($H_{2,15} = 7.3$, $p = 0.02$) and ZpFLM ($H_{2,15} = 9.2$, $p = 0.01$). When animals were allowed to drink (DPAT + W), c-Fos activity increased in the nucleus raphe pontis ($F_{2,12} = 11$, $p = 0.001$) and the LC (Fig. 8). In Anl and ZpFLM, allowance of water intake decreased the effect of DPAT injection on the number of c-Fos+ cells ($p < 0.002$ for DPAT vs. DPAT + W, Mann–Whitney post hoc test for both nuclei) (Fig. 8). The density of double-labeled cells was increased in the LC, Anl and ZpFLM in both DPAT-treated groups. ANOVA did not indicate any significant effect of DPAT injection on TPH labeling among the different groups (Fig. 8). No change in the number of

Table 2
Effects of the neurotoxin 5,7-DHT on the 5-HT levels in different areas of the pigeon brain ($n = 6$/experimental group). The values are presented as the % of the values in the control animals. The (−) symbol in front of a number indicates a reduction. The data are expressed as the medians ± interquartile range.

Groups	Brainstem	Hypothalamus	Hippocampo	Arcopalium
Sham 12	−3.9 ± 14.2	−2.1 ± 53.1	−1.4 ± 38.8	−2.5 ± 24.5
Sham 28	−1.8 ± 13.3	−2.6 ± 86.8	18.3 ± 39.4	−0.5 ± 58.6
DHT 12	−56.6 ± 10.5*	−80.08 ± 33.2*	−66.4 ± 35.6*	−0.18 ± 45.4
DHT 28	−64.8 ± 7.2*	−70.1 ± 22.4*	−40.4 ± 20.6*	36.7 ± 25.2

* $p < 0.05$ compared to the control untreated animals (set as 100%, data not shown).

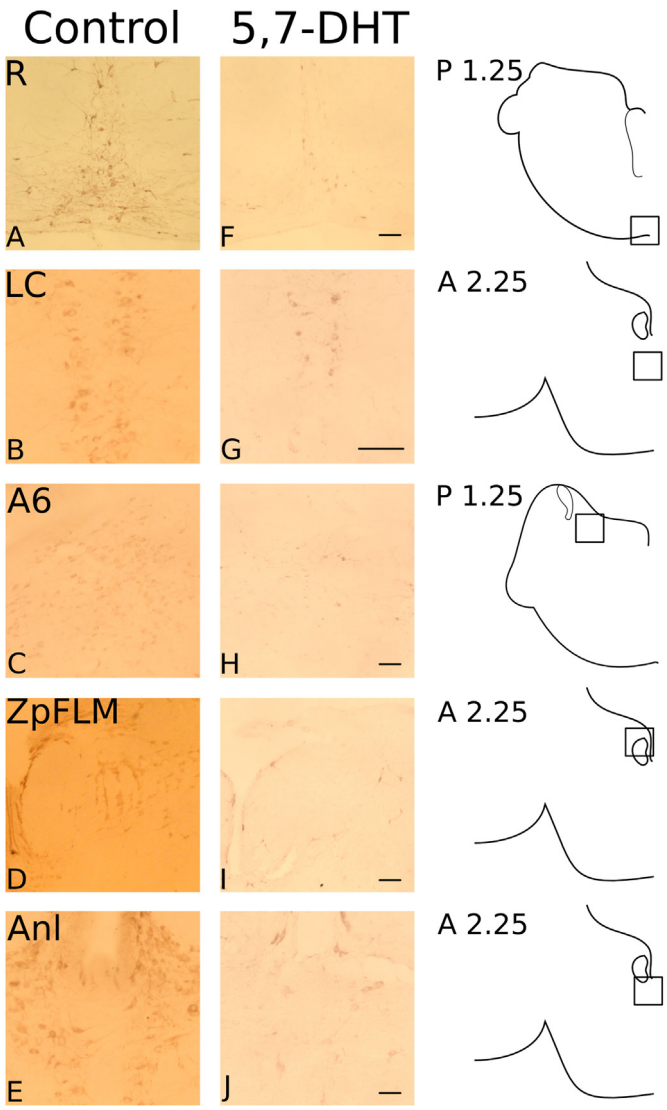

Fig. 6. Effects of 5,7-DHT injections on the density of TPH-immunoreactive cells in brainstem nuclei containing 5-HT neurons ($N = 6$). Left two columns: photomicrographs of control untreated animals (panels A–E) and animals injected ICV with 5,7-DHT (panels F–J). Right column: schematic drawings of frontal sections of the pigeon brain showing the anatomical location of the analyzed structures. The alphanumeric characters placed at the upper left corner indicate the approximate stereotaxic levels according to the Karten and Hodos atlas [44]. Scale bar = 100.

c-Fos+ or double-labeled cells in area A6 or A8 was detected (data not shown).

3.5. *Effects of DPAT and 5-HT ICV injection on c-Fos activation in the hypothalamus and in prosencephalic periventricular areas*

DPAT injection increased c-Fos labeling in the subfornical organ (SFO: $H_{2,15} = 9.4$, $p = 0.009$), the preopticus medialis (POM: $F_{2,12} = 12.5$, $p = 0.002$), the preopticus anterior (POA: $F_{2,12} = 27$, $p < 0.0003$) (Table 3), the dorso medialis hypothalami (DMN: $F_{2,12} = 26$, $p < 0.001$), the ventro medialis hypothalami (VMN: $F_{2,12} = 34$, $p = 0.001$) and in the LHy ($F_{2,12} = 21$, $p = 0.001$) (Fig. 9). DPAT also increased the number of c-Fos+ cells in bed nucleus of the stria terminalis pars lateralis (BNSTl: $H_{2,15} = 12$, $p = 0.002$) and in septal lateral areas (SL: $H_{2,15} = 93$, $p < 0.0001$) (Table 3). In the animals allowed to drink after DPAT injection, we detected an increase in the number of c-Fos+ cells in the SFO ($H_{2,15} = 9.4$, $p = 0.009$), the PVN ($H_{2,15} = 7.9$, $p = 0.001$) and the POA (Table 3; Figs. 9 and 10). In the SL and the POM, the effects of DPAT on c-Fos expression were increased after water intake (post hoc analysis, $p < 0.001$ for DPAT vs. DPAT + W for both nuclei) (Table 3). Conversely, a decrease in DPAT-induced c-Fos+ cells was detected in the BNSTl after water intake (Mann–Whitney U test, $p = 0.009$) (Table 3). In the PVO ($F_{2,12} = 48.1$ $p < 0.0001$) and the PVN, we detected an increase in c-Fos+ cells only in the animals that were allowed to drink after injection (Fig. 9; Table 3).

5-HT increased the number of c-Fos+ cells in almost all hypothalamic nuclei examined (PVO: $F_{2,12} = 9.4$, $p = 0.02$; SFO: $H_{2,15} = 14$, $p = 0.002$; PVN: $H_{2,15} = 21$, $p = 0.001$; POM: $F_{2,12} = 37$, $p = 0.001$; and POA: $F_{2,12} = 18$, $p = 0.002$) (Table 3). Moreover, 5-HT increased the number of c-Fos+ cells in the SL ($H_{2,15} = 12{,}5$, $p = 0{,}002$) and the BSTNl ($H_{2,15} = 37.3$, $p < 0.0001$). Water intake decreased the effect of 5-HT on c-Fos activity in the SL, the BSTNl and the POM and blocked the 5-HT-mediated increase in the number of c-Fos+ cells in the PVO and the SFO (Fig. 9; Table 3). However, 5-HT injection decreased the number of c-Fos+ cells in the DMN ($F_{2,12} = 14$, $p < 0{,}03$) and the LHy ($F_{2,12} = 16$, $p < 0{,}05$) (Fig. 9).

4. Discussion

The present data indicate that 5-HT$_{1ARs}$ are densely concentrated in the brainstem and in the periventricular preoptic-hypothalamic areas of the pigeon brain, extending previous findings that these receptors are widely distributed in the pallial and pretectal/tectal regions in this species [33]. The radioligand [^{3}H]-8-OH-DPAT appeared to bind most strongly to post- and pre-synaptic 5-HT$_{1ARs}$; DPAT is a highly specific 5-HT$_{1AR}$agonist [58,59,60] that has been used as a radioligand to determine the distribution of 5-HT$_{1ARs}$ in various vertebrate species [61,27,54,62–65]. However, DPAT also displays moderate affinity for the 5-HT$_{7R}$ subtype (in guinea-pig: [66,67]), rat and human

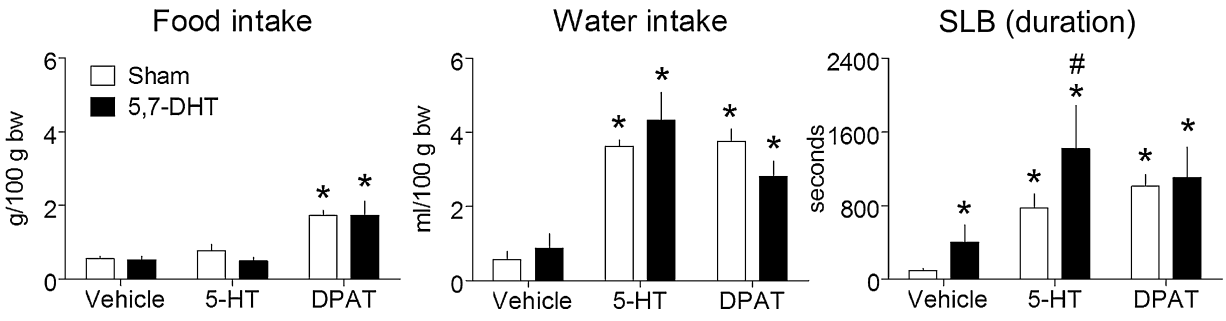

Fig. 7. Effects of ICV injection of 5-HT (150 nmol) or DPAT (30 nmol) on food and water intake and SLB after pre-treatment with 5,7-DHT or vehicle (Sham; $N = 6$/experimental group). The data are expressed as the means ± S.E.M. $^*p < 0.05$ compared to sham animals treated with vehicle; $^\#p < 0.05$ compared to sham animals treated with 5-HT.

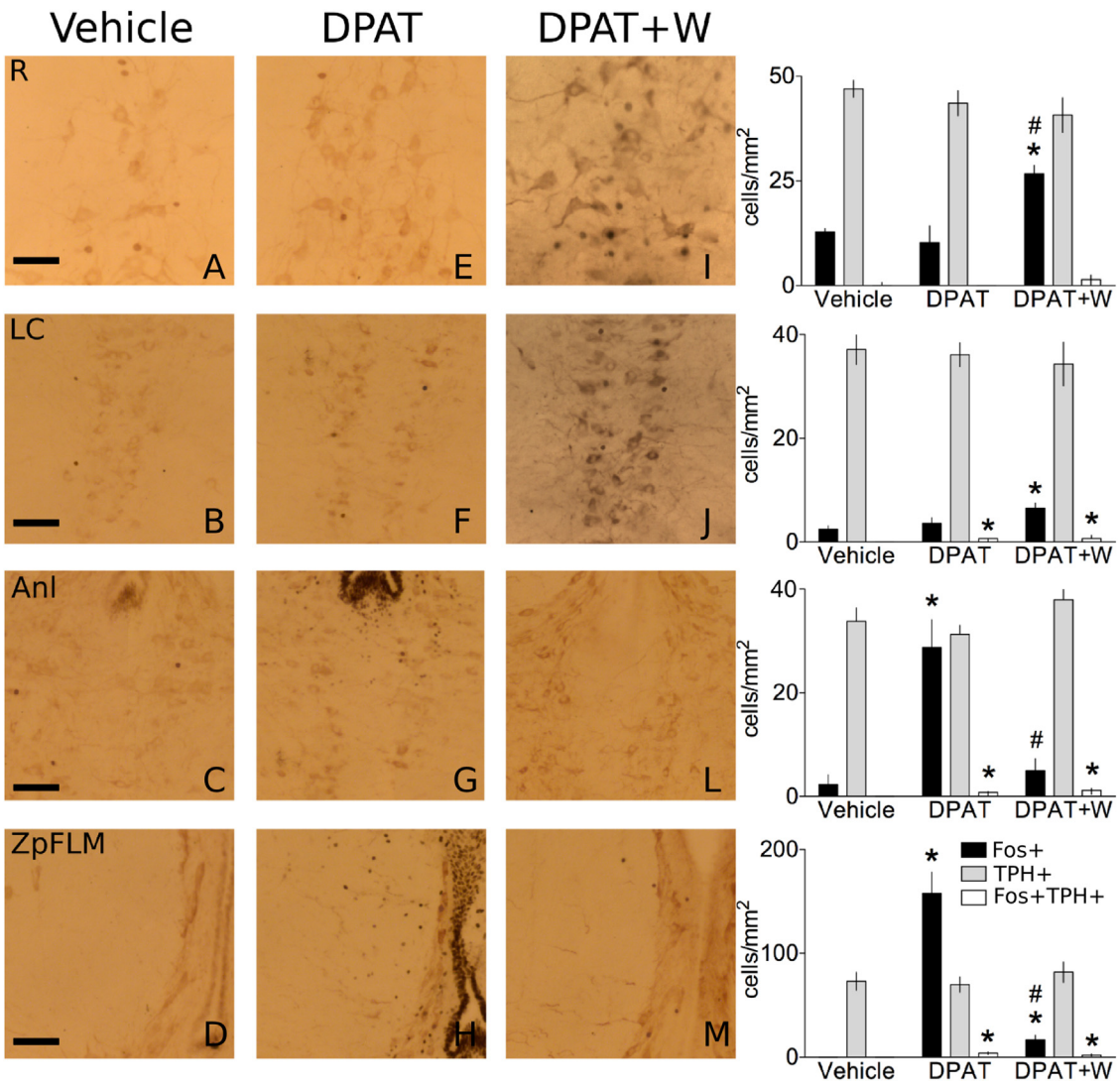

Fig. 8. Representative photomicrographs showing the effects of ICV injection of DPAT (30 nmol) on the number of c-Fos+, TPH+ and double-labeled cells in brainstem nuclei ($N = 8$/experimental group). DPAT-injected animals were provided with no (DPAT; panels E–H) or with free access to water (DPAT + W; panels I–M) after injection. $^{*}p < 0.05$ compared to the vehicle group (panels A–D). Scale bar = 100 μm. $^{\#}p < 0.05$ compared to DPAT. The c-Fos countsin the R nucleus and the LC are expressed as the means ± S.E.M. The c-Fos counts in AnI and ZpFLM and all TPH+ and double-labeled cells are expressed as the medians ± interquartile range. For abbreviations, see the list.

brain tissue [68]. To avoid the binding of [^{3}H]-8-OH-DPAT to 5-HT$_{7Rs}$, we used a concentration that does not bind to 5-HT$_{7Rs}$ in 5-HT$_{1AR}$ knockout mice. Bonaventure and colleagues [69] demonstrated that 1 or 2 nmol [^{3}H]-8-OH-DPAT does not bind or displays a very low binding density in the septal area of knockout mice compared to the moderate to high binding densities in the area of wild-type animals [69]. Consistently, lower K_D values (1.3 nM, 95% confidence interval 0.35–2.25 nM) were obtained in the septum of wild-type animals than in that of knockout animals (5-HT$_{1AR}$ knockout animals: 20 nM, 95% confidence interval 14–27 nM). At 10 nM [^{3}H]8-OH-DPAT, high densities were detected in both wild-type and 5-HT$_{1AR}$ knockout mice [69], suggesting that at higher doses than the one used in this study, DPAT binds to receptors other than 5-HT$_{1ARs}$.

Table 3
Effects of ICV injection of vehicle, DPAT (30 nmol) or 5-HT (150 nmol) on c-Fos protein expression in hypothalamic nuclei (PVO, SFO, PVN, POM and POA) and in the SL and the BNSTl ($N = 8$/experimental group). The symbol +W indicates the animals treated with DPAT or 5-HT that were provided with free access to water after injection. Vehicle-treated animals also received free access to water for all experiments. For the structure names, see Table 1. The data for the SFO, the PVN, the BNSTl and the SL are expressed as the medians ± interquartile range. For abbreviations, see the list.

Groups/nuclei	PVO	SFO	PVN	BSTNl	SL	POM	POA
Vehicle	7 ± 1.4	17.6 ± 4.5	56.4 ± 5.9	21.8 ± 4.2	9 ± 1.2	9.6 ± 1.3	4.8 ± 1.4
DPAT	14.4 ± 2	123 ± 16*	71.6 ± 8.6	421 ± 36*	346 ± 25*	30.4 ± 3.6*	40.4 ± 3*
DPAT + W	57.6 ± 8*,#	128 ± 10*	120 ± 3*,#	79.2 ± 6.2*,#	786 ± 65*,#	117 ± 9*#	27.6 ± 5*
5-HT	26 ± 5.5*	60.2 ± 7.3*	137 ± 3*	118 ± 11*	835 ± 100*	108 ± 11*	24.6 ± 3.3*
5-HT + W	4.4 ± 1.4#	24.2 ± 5.7#	153 ± 5*	86.2 ± 6.6*,#	285 ± 37*,#	56 ± 8*#	34 ± 4.8*

* $p < 0.05$ compared to the vehicle group.
# $p < 0.05$ for DPAT vs. DPAT + W or 5-HT vs. 5-HT + W.
The c-Fos counts in the PVO, the POM and the POA are expressed as the means ± S.E.M.

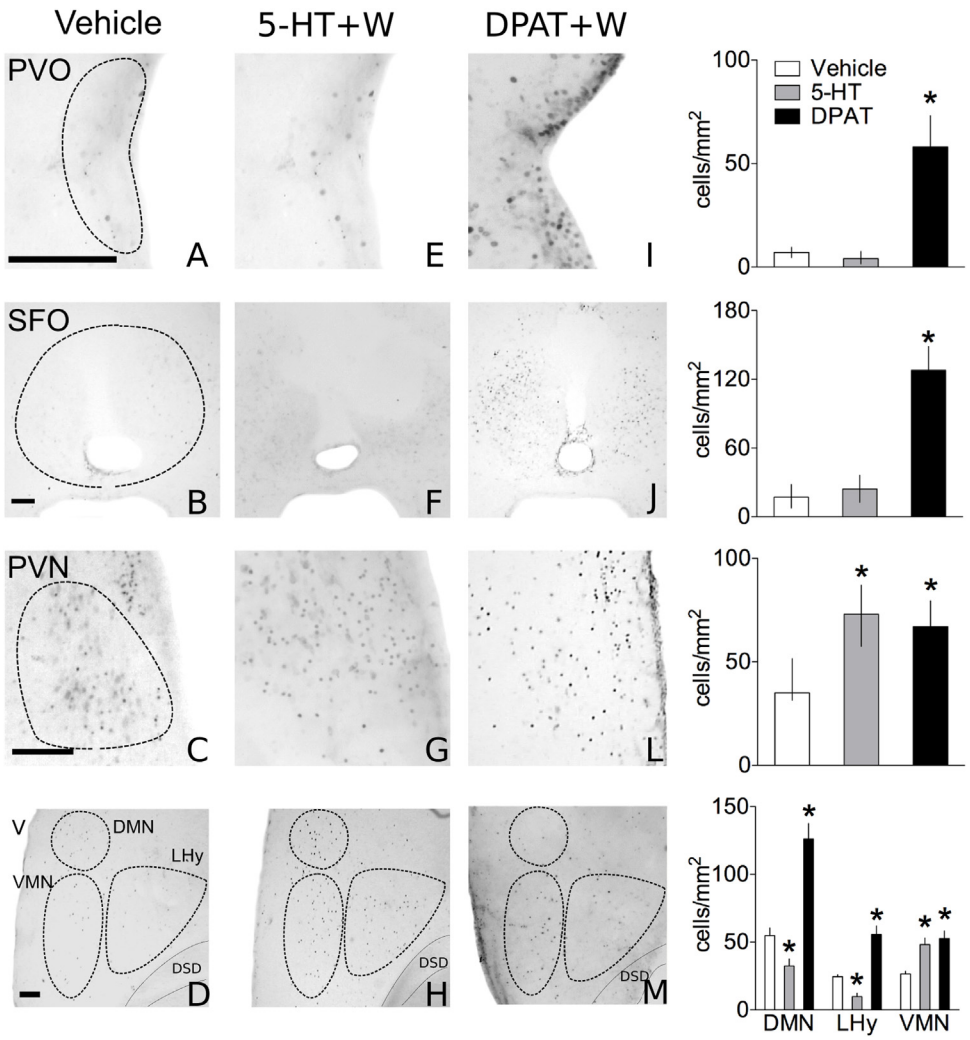

Fig. 9. Representative photomicrographs showing the effects of ICV injection of 5-HT (150 nmol) or DPAT (30 nmol) on the number of c-Fos+ cells in hypothalamic nuclei: vehicle group (panels A–D); 5-HT + W group (panels E–H);and DPAT + W group (panels I–M; $N = 6$/experimental group). All animals were provided with free access to water after injection. $^{*}p < 0{,}05$ compared to the vehicle group. Scale bar = 100 μm. The c-Fos counts for the PVO, the VMN, the DMN and the LHy are expressed as the means ± S.E.M. The data for the SFO and the PVN are expressed as the medians ± interquartile range. For abbreviations, see the list.

In those pontomesencephalic areas that were examined, [^{3}H]-8-OH-DPAT binding was localized to nuclei previously reported to contain high concentrations of 5-HT-immunoreactive cell bodies in pigeons, chickens and quails (e.g., [70–73,14]) and TPH (the rate-limiting enzyme in the biosynthesis of 5-HT)-immunoreactive cell bodies in pigeons [46,12]. These nuclei (R, Anl, ZpFLM, LC, A6 and A8) constitute the rostral or superior raphe nuclei in birds; areas A6 and A8 in pigeons also contain dense populations of dopaminergic (A8) or noradrenergic (A6) neurons [74,75] that appear to partially overlap with the serotonergic perikarya. Dense populations of 5-HT_{1ARs} are found in the raphe nuclei are comparable to those in mammals (rodents: [28,38]); humans: [76]. In the mammalian midbrain raphe nuclei, 5-HT_{1ARs} control 5-HTergic neuron firing and 5-HT release [77–79], acting as somatodendritic autoreceptors to inhibit 5-HTergic neuron firing and release upon stimulation with endogenous 5-HT or 5-HT_{1AR} agonists. These 5-HT_{1ARs} are not tonically activated by endogenous 5-HT under resting, physiological conditions, but 5-HT_{1ARs} can inhibit the 5-HTergic neuron firing rate and 5-HT efflux in response to endogenous 5-HT surges evoked by changes in the behavioral state of the animal [80–82].

In pigeons, systemic injection of DPAT decreases the levels of 5-HIAA (a 5-HT metabolite) but does not change the levels of other monoaminergic metabolites in the cerebrospinal fluid (CSF) [22,23,83], suggesting that in this species, this 5-HT_{1AR} agonist decreases the activity of 5-HTergic neurons. The 5-HIAA levels in the mammalian ventricular CSF have been shown to reliably indicate serotonergic activity in the brain (e.g., [84]). Along these lines, it is interesting that ICV 5-HT injection into pigeons *reduced* c-Fos expression in TPH+ neurons in the LC and areas A6 and A8 but not in the pontine raphe nucleus [12]. These results suggest that, although the precise cellular localization of these binding sites cannot be determined based on the autoradiography method used here, the observed labeling may be at least partially associated with somatodendritic inhibitory 5-HT_{1ARs} on serotonergic neurons in the raphe nuclei.

However, it appears that inhibition of 5-HTergic neurons due to activation of somatodendritic 5-HT_{1ARs} is not sufficient to account for the acute neural and behavioral effects of ICV 5-HT or DPAT injection. Injection of DPAT produced a modest increase in the number of c-Fos+ (in Anl and ZpFLM) and c-Fos+/TPH+ cells (in the LC, Anl and ZpFLM, present data) predominantly in the *animals that were allowed to drink*. Alternatively, ICV 5-HT injection consistently *reduced* the number of c-Fos+/TPH+ neurons when the animals *were not allowed* to drink [12]. These data suggest that 5-HTergic neuronal activity in the raphe nuclei tends to increase slightly or return to basal levels when the animal satisfies its 5-HT- or DPAT-evoked

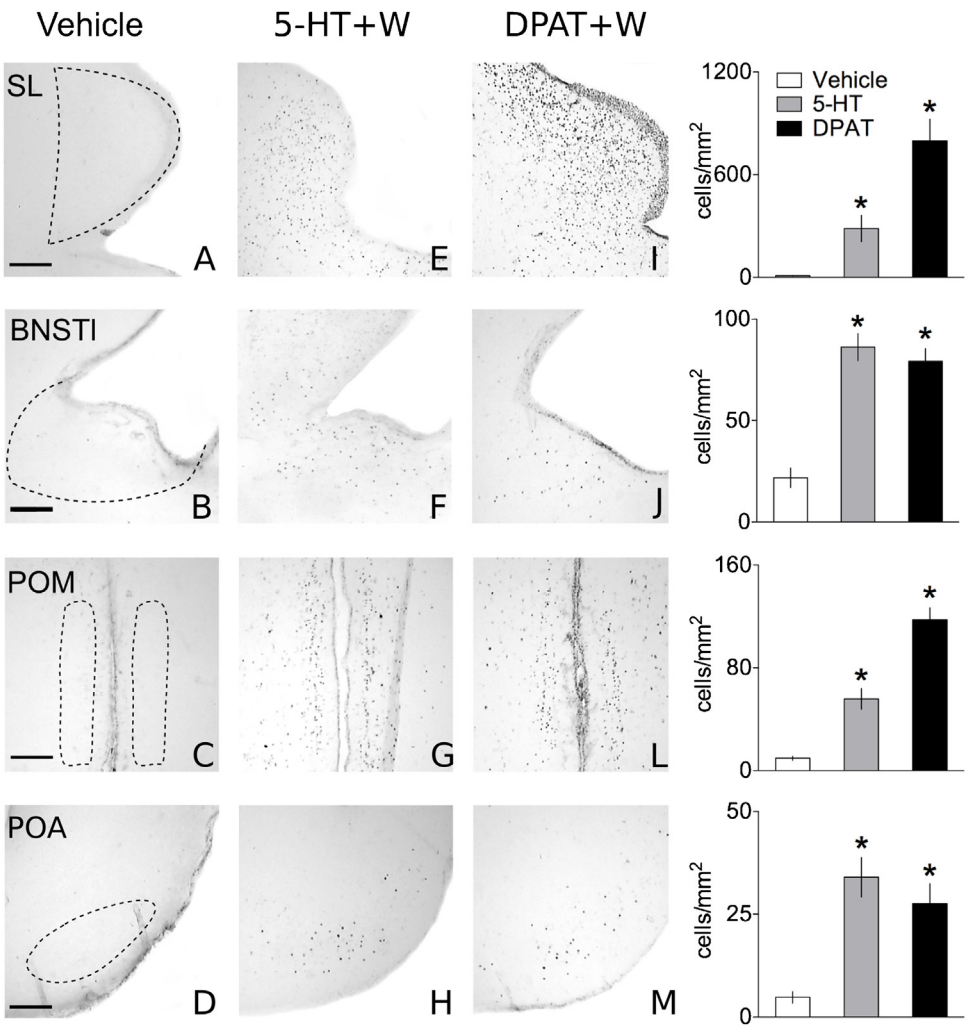

Fig. 10. Representative photomicrographs showing the effects of ICV injection of 5-HT (150 nmol) or DPAT (30 nmol) on the number of c-Fos+ cells in the hypothalamic nuclei: vehicle group (panels A–D); 5-HT + W group (panels E–H); and DPAT + W group (panels I–M; $N = 6$/experimental group). All animals were provided with free access to water after injection. Scale bar = 100 μm. $^{*}p < 0.05$ compared to the vehicle-treated group. The c-Fos counts in the POM and the POA are expressed as the means ± S.E.M. The data for the BNSTl and the SL are expressed as the medians ± interquartile range. For abbreviations, see the list.

search for water and that the reduced activity of 5-HTergic neurons in the raphe nuclei may be associated with a thirst-like state or may be associated to the act of drinking per se.

Furthermore, bilateral ICV injection of 5,7-DHT (200 μg/ventricle) decreased the 5-HT levels in the upper brainstem, the hypothalamus and the hippocampus and reduced the number of TPH+ neurons in the raphe nuclei. Our findings differed quantitatively from those of a previous study that administered the same toxin to pigeons [37]. They performed a single intra-aqueductal injection of 5,7-DHT (600 μg), and 9 and 60 days after injection, they detected a decrease in the 5-HT levels in a pallial visual area (the Wulst) and in the optic tectum but not in the brainstem. The causes of these conflicting results remain unclear, but they may be related to the differences in the injection volume/site or the different size and rostrocaudal span of the brainstem samples examined; they used 5.5 mm long samples from the caudal medulla oblongata (P3.00) to the rostral pontine levels (A2.50), whereas we sampled only the rostral pons (between A1.00 and A2.25 levels). In rodents, intense reductions in TPH activity and the 5-HT levels in the hippocampus and cerebral cortex and decreases in [^{3}H]-8-OH-DPAT binding exclusively in the midbrain raphe nuclei were detected after intracerebral injection of 5,7-DHT (e.g., [38]). Intracisternal [85] or intra-raphe nuclear (median or dorsal; [40]) injection of 5,7-DHT impaired feeding induced by systemic injection of DPAT, suggesting that DPAT-induced feeding is dependent on activation of somatodendritic, inhibitory 5-HT$_{1ARs}$ in rats.

Conversely, and despite the apparently intense and selective 5,7-DHT-induced reduction in 5-HT activity in our pigeons, the ingestive and hypnogenic effects of 5-HT and DPAT ICV injection were not changed in the 5,7-DHT-treated animals. These results may indicate that drinking and sleep induced by DPAT and 5-HT, as well as hyperphagia induced by DPAT, are not dependent on a reduction in the activity of the central 5-HTergic circuitry mediated by activation of inhibitory somatodendritic 5-HT$_{1ARs}$ in pigeons. In fact, 5,7-DHT-induced lesion increased sleep duration in both the vehicle- and 5-HT-treated animals, suggesting that a chronic reduction in brain 5-HT activity induces plastic changes in sleep-related circuits, leading to sleepiness and an increased susceptibility to the sleep-evoking effects of 5-HT. We have shown that ICV injection of DPAT or 5-HT increases the duration of electrographically characterized desynchronized sleep (or rapid-eye-movement, REM) and slow wave sleep (SWS) based on hippocampal EEG recordings [13].

In mammals, sleep states have been associated with decreased activity or inactivity of serotonergic neurons (compared to wakefulness). Dorsal raphe neurons fire intensely during wakefulness

but exhibit decreased firing during SWS and cease firing during REM sleep [17,18]. Perfusion of the dorsal raphe nucleus with DPAT decreased 5-HT release and increased REM sleep in cats [21] and rats [86], indicating that a somatodendritic 5-HT_{1AR}-mediated decrease in the activity of serotonergic neurons is associated with this sleep state. Interestingly, similar to the findings in pigeons [13], sleep and electroencephalographic activity typical of SWS was detected after ICV injection of low doses of 5-HT into mammals [19,87]. The role of 5-HT_{1ARs} has been studied via systemic and intra-raphe injection of the 5-$HT_{1A/7R}$ agonist DPAT. In free-feeding rats, DPAT increases food intake when administered systemically [88,89] or into the dorsal or median raphe nuclei [34,90], and these effects are most likely dependent on the activation of somatodendritic, inhibitory 5-HT_{1ARs} in rats [85,40]. Thus, it appears that DPAT-induced hyperphagia, as well as DPAT- and 5-HT-induced sleep, depend on distinct 5-HT_{1AR}-mediated mechanisms in mammals and pigeons.

We have previously shown that ICV pretreatment with low doses of the 5-HT_{1AR} antagonist WAY100635 attenuates the dipsogenic and hypnogenic effects of low doses of 5-HT (50 nmol), and reduced the DPAT-evoked increases in feeding, drinking and sleep in pigeons [13], confirming that these effects may be dependent on the activation of 5-HT_{1ARs}. WAY100635 displays high affinity for 5-HT_{1ARs} (K_i = 4.5 nM) and antagonist-like activity on both presynaptic and postsynaptic 5-HT_{1ARs} [91,92,35]. Here, we further explored the effects of 5-HT_{1AR} antagonists by injecting MM77 (an agent that acts primarily on postsynaptic 5-HT_{1ARs}) before ICV injection of 5-HT or DPAT. MM77 is characterized as a postsynaptic 5-HT_{1AR} antagonist [43], and its antagonistic effect on postsynaptic 5-HT_{1ARs} has been described [93,45]. In one study [94], the anti-conflict effects of WAY100636 and MM77 were compared in rats whose 5-HTergic neurons were destroyed by prior administration of p-chloroamphetamine (which reduced the hippocampal concentration of 5-HT by ca. 85%). In these animals, the anti-conflict effect of WAY100635, but not MM77, was abolished, indicating that the anxiolytic-like activity of MM77 does not appear to depend on the integrity of presynaptic 5-HT_{1ARs}. The present data indicate that pretreatment with MM77 reduces 5-HT-induced drinking and both 5-HT- and DPAT-induced sleep. If MM77 indeed acts preferably at postsynaptic 5-HT_{1ARs} in pigeons, these results reinforce the concept that the somatodendritic 5-HT_{1AR}-mediated decrease in the activity of serotonergic neurons is of little relevance to these 5-HT-evoked behavioral effects. Surprisingly, MM77 failed to affect DPAT-induced feeding or drinking, indicating that WAY100635 (which attenuated these DPAT-induced responses) and MM77 may display distinct pharmacological profiles with respect to their interactions with DPAT-sensitive receptors.

Beyond the likely expression of somatodendritic 5-HT_{1ARs} on serotonergic neurons in the raphe nuclei, our autoradiographic data indicate that 5-HT_{1ARs} (pre- and/or post-synaptic) are especially concentrated in periventricular hypothalamic and preoptic areas and in the circumventricular organs. These dense [^{3}H]-8-OH-DPAT binding patterns agree with the evidence for dense serotonergic innervation of these medial/paraventricular hypothalamic regions in pigeons [72] and for 5-HT+ and TPH+ cell clusters in the cerebrospinal fluid (CSF)-contacting neurons of circumventricular areas (in the hypothalamic recessus infundibularis, in the PVO and in sub- and supra-ependymal patches in aqueductal levels and throughout the lateral and third ventricles; [95,73,46]) of the pigeon. Furthermore, the medial preoptic nucleus, the anterior-medial hypothalamic area, including the paraventricular and the posteromedial hypothalamic nucleus, have been shown to be extensively inter-connected [96–98] in pigeons. Efferent from these regions innervate the septal lateral, posterior hypothalamic and medial mammillary areas, the median eminence and neurohypophysis, as well as the brainstem, whereas afferent input to these regions originates from CSF-contacting cells (including 5-HT+ neurons), circumventricular organs (SFO, OVLT, area postrema), and limbic and autonomic areas of the brainstem and the prosencephalon in birds. Thus, these periventricular preoptico-hypothalamic receptors are positioned to mediate the important serotonergic functions in reproductive and chronobiologically dependent states (e.g., [99]), in sleep [100,101], in the control of thermal and fuel-related metabolism [100,102,103], and in the performance of ingestive behaviors [103,10,104,12,13], as suggested by local, ICV and systemic injection of 5-HT or drugs that interact with 5-HT_{1ARs} in pigeons and chickens.

The [^{3}H]8-OH-DPAT labeling patterns described here and by Herold and colleagues [33] are in line with the intense c-Fos labeling induced by 5-HT or DPAT ICV injection in these preoptic-hypothalamic periventricular regions and in the SL and the BNSTl. 5-HT injection increased the number of c-Fos+ cells in the parenchyma (PVN, BNSTl, SL, POM and POA) the circumventricular organs (PVO, SFO), which were, exception for the PVN, *attenuated or abolished by drinking*. These data suggest that the 5-HT-induced increase in c-Fos expression in these nuclei may be associated with thirst-related phenomena, whereas that in the PVN may be related to other 5-HT-induced functions. Interestingly, injection of metergoline (an antagonist of 5-$HT_{1/2Rs}$) or GR-46611 (a 5-$HT_{1B/1DR}$ agonist) into the PVN, the posterior medial hypothalamus and the caudal preoptic region evoked feeding without changing water intake in free-feeding pigeons [10], indicating that 5-HT-induced c-Fos activity in the PVN may be related to a 5-HT_{1BR}-mediated effect of 5-HT on feeding behavior. The number of c-Fos+ cells was increased in the PVN, the medial preoptic area, the SFO and the SL of chickens, quails, zebra finches and starlings that had been injected intraperitoneally with hypertonic saline 3 h earlier [105], which increased drinking behavior and the plasma vasotocin and angiotensin II levels in birds [106]. Hypertonic saline-induced c-Fos labeling was shown to co-localize with vasotocin-immunoreactive neurons in the PVN (in magnocellular cells known to project to the neurohypophysis), in the posterior hypothalamus and in the ventral floor of the rostral preoptic area. These data may underscore the relevance of serotonergic mechanisms to hypothalamic that regulate the hydrosaline balance in birds.

Interestingly, DPAT injection altered c-Fos expression in the same regions that were reactive to 5-HT injection, although in a different (even divergent) pattern: the number of c-Fos+ neurons was *increased* in the PVO, PVN, SL and POM among animals allowed to drink. These data suggest that these effects of DPAT on c-Fos expression in these nuclei may be associated with the drinking behavior itself, to the satiation of DPAT-induced thirst, or to other DPAT-induced effects (including hyperphagia and sleep). In addition, the complex pattern of c-Fos activity produced by DPAT injection in hypothalamic areas, in contrast to the limited level of c-Fos activation in serotonergic brainstem areas, contributes to the concept that heterosynaptic or non-somatodendritic presynaptic 5-HT_{1ARs} are crucial for the dipsogenic and hypnogenic effects of 5-HT. Moreover, the differences in c-Fos activity between the 5-HT- and DPAT-injected animals indicate that 5-HT receptors other than 5-HT_{1ARs} also participate in the functions mediated by hypothalamic serotonergic circuits.

The distribution of hypothalamic [^{3}H]-8-OH-DPAT-binding sites in the pigeon is comparable to that in the rodent brain [28,69], including intense expression in the choroid plexus and moderate expression in the paraventricular, dorsomedial, ventromedial, posterior, anterior, mammillary and arcuate nuclei, as well as the preoptic area. The ventromedial, lateral, anterior, and dorsomedial hypothalamus and the paraventricular, magnocellular preoptic and supraoptic nuclei contain cells and cellular processes displaying 5-HT_{1AR}-like immunoreactivity [107,31,32]. Many of these cells also display immunoreactivity to sleep- and feeding-related

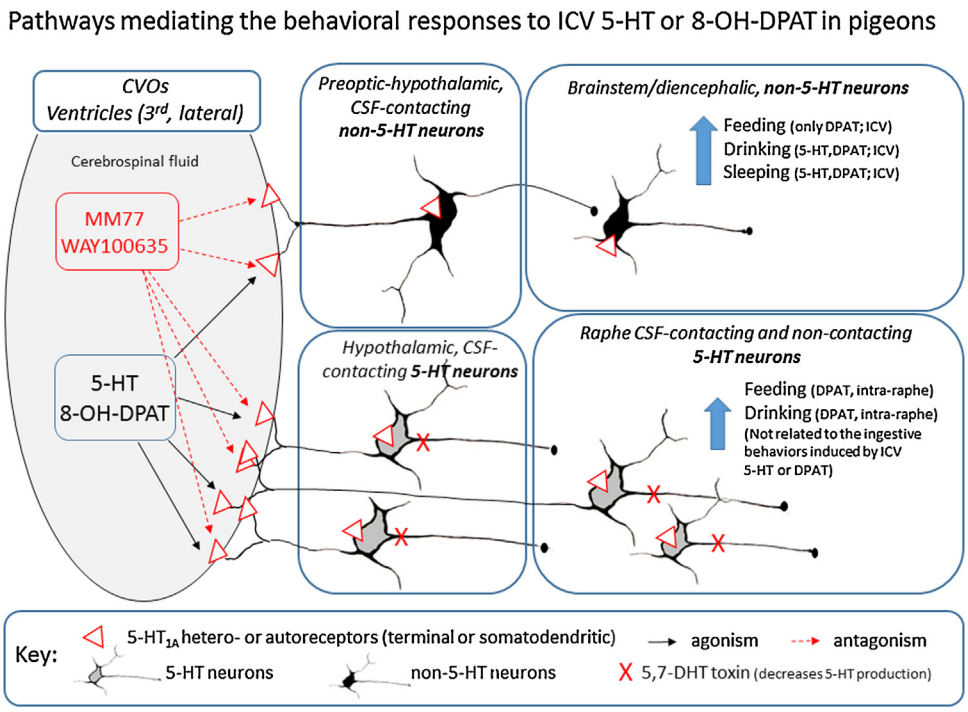

Fig. 11. Schematic diagram summarizing the rationale of the experiments and the main findings of the present report, and showing the putative brain circuits involved in organizing behavioral responses to ICV injections of 5-HT and 8-OH-DPAT in pigeons. As indicated by [^{3}H]8-OH-DPAT labeling, 5-HT1A hetero- or autoreceptors (terminal or somatodendritic) are localized in brainstem raphe, rich in 5-HT-producing neurons, as well as in circumventricular organs (CVOs) and periventricular preoptico-hypothalamic regions. Some of these regions are endowed with cerebrospinal fluid (CSF)-contacting serotonergic and non-serotonergic neurons. ICV injections of 5-HT [13] or 8-OH-DPAT (5-HT1AR agonist; present results) changes c-Fos expression in these regions, and evokes prompt and intense drinking, sleeping and feeding (for 8-OH-DPAT only) responses in free-feeding pigeons. These behavioral responses are blocked by WAY-100635 (5-HT 1AR antagonist of hetero and autoreceptors [13]) and by MM77 (5-HT 1AR antagonist at heteroreceptors; present results). ICV injection of the toxin 5,7-DHT, which decreased the 5-HT levels in the upper brainstem and the hypothalamus and reduced the number of 5-HT-producing neurons in the raphe nuclei, left unchanged the behavioral responses to ICV 5-HT or 8-OH-DPAT. These evidence suggest that the behavioral responses to ICV 5-HT and DPAT are mediated by 5-HT1AR heteroreceptors located at CVOs or diencephalic, CFS-contacting, non-serotonergic neurons and circuits, while 5-HT neurons and circuits located in the hypothalamus or in the raphe nuclei are not involved in these responses. The latter may be also involved in circuits controlling ingestive behaviors, since intra-raphe 8-OH-DPAT injections evoke feeding and drinking in this species [14].

peptides (neuropeptide Y, agouti-related peptide, cocaine- and amphetamine-regulated transcript, melanin-concentrating hormone and orexin; [31]). These results suggest that serotonin acts via postsynaptic 5-HT$_{1ARs}$ to influence the release of feeding-regulated peptides. In line with this hypothesis, it was found that local injections of DPAT into the lateral, arcuate [108,109] and PVN [110] evoked hypophagia in rats. At least in the lateral hypothalamus and the arcuate nucleus, this effect of DPAT was blocked by pretreatment with WAY100635 [108,109].

The massive accumulation of [^{3}H]-8-OH-DPAT labeling and 5-HT-induced c-Fos reactivity in the periventricular hypothalamic and septal areas containing CSF-contacting neurons may indicate an important role of the ventricular wall and intraventricular 5-HT levels in regulating sleep, feeding and drinking in pigeons. 5-HT-immunoreactive processes containing dense core vesicles invade and heavily populate the ventricular ependymal lining in all vertebrate species examined to date [111,112,95,113,114], and 5-HT+ cells in the PVO and the posterior hypothalamic recess extend processes that protrude into the ventricular lumen and that proceed ependymofugally in all studied non-mammalian species [95,114], including the pigeon [73,46]. Some of these CSF-contacting PVO cells also display TPH immunoreactivity and, thus, may produce 5-HT [46]. Therefore, these subependymal CSF-contacting elements are positioned to synthesize/release 5-HT into the CSF. Some of these cells are also influenced by the intra-CSF 5-HT levels via 5-HT$_{1AR}$ activation [115,114]. The circumventricular organs were repeatedly shown to be associated with both blood- and CSF-borne substances to regulate a variety of functions, including feeding, drinking and circadian sleep regulation (e.g., [116–119]). However, since 5,7-DHT treatment decreased brainstem and hypothalamic 5-HT, but failed to affect the 5-HT$_{1AR}$-mediated, 5-HT behavioral responses to intraventricular 5-HT and DPAT, the fluid-contacting serotonergic neurons (located either in the raphe nuclei or in the periventricular diencephalon) may not be directly responsible for the 5-HT-evoked responses. Thus, it is conceivable that non-serotonergic neurons endowed with 5-HT$_{1A}$ receptors, located in circumventricular organs or parenchymal hypothalamus, with CSF-contacting processes, may constitute the circuit through which ventricular 5-HT influences ingestive and sleep behaviors in pigeons (Fig. 11). The mechanisms controlling the 5-HT content of the CSF, which are located upstream to these non-serotonergic circuits, are unknown and warrant further investigation. Furthermore, these data suggest that the changes in the c-Fos+/TPH+ neurons observed after intraventricular 5-HT and DPAT injections may not be associated to the behavioral effects of these treatments examined in the present report.

Central 5-HT circuits display neurochemical and neuroanatomical characteristics that appear to be highly conserved in vertebrates [120–122]. The present data indicate that the distribution of 5-HT$_{1ARs}$ in the brainstem raphe nuclei and in the periventricular diencephalic structures is comparable to that found in mammals and suggest that 5-HT circuits and 5-HT$_{1ARs}$ play important functional roles in the performance of ingestive and sleep behaviors in an avian species, in parallel with the findings in mammals. However, despite these similarities, the mechanisms by which these circuits generate these similar behavioral effects may depend on distinct or opposing neurobiological mechanisms between rodents (somatodendritic autoreceptor-related) and pigeons

(heterosynaptic- or non-somatodendritic autoreceptor-related). It is conceivable that species- (or taxa-) specific attributes of central 5-HTergic mechanisms co-exist with phylogenetically ancient traits. Further comparative studies of the functional roles of 5-HTergic circuits may discriminate the primitive or shared functional characteristics (that may be of general relevance for vertebrates or result from convergent evolutionary mechanisms) from those which are unique to a given taxon.

Conflict of interest statement

All authors state that they have no actual or potential conflict of interest, including any financial, personal or other relationship with other individuals or organizations that could inappropriately influence the work submitted here.

Role of the funding source

The funding agencies, including CNPq, Capes, FAPESC and DFG, had no influence or role in the study design, in the collection/analysis/interpretation of the data, in the writing of the report, or in the decision to submit the paper for publication.

Authors contribution

Tiago Souza dos Santos: behavioral experiments and design, collection and analysis of behavioral data; writing the manuscript; Jéssica Krueger: behavioral experiments; collection of the neurochemical and behavioral data; Fernando Falkenburger Melleu: collection and analysis of behavioral data; Anicleto Poli: collection and chromatographic analysis of neurochemical data; Christina Herold: autoradiography procedures and image processing; Karl Zilles: experimental design, approval of the final version of the article; Onur Güntürkün: experimental design, approval of the final version of the article; José Marino Neto: experimental design, selection of the theme, data analysis, writing the paper, approval of the final version of the article.

Acknowledgments

This study was supported by CNPq and FAPESC research grants to J. Marino-Neto (proc. 471888/03-6 and 300308/2007-8) and by DFG via grants FOR1581 and SFB874 to O. Güntürkün. F. Melleu and T.S. dos Santos received Graduate (PhD) fellowships from Capes. T.S. dos Santos also received a PhD sandwich fellowship from the CNPq "Science without Borders" Program. J. Kruger received a PIBIC-CNPq undergraduate research fellowship. We wish to thank the helpful comments and suggestions made by Dr. Cilene Lino-de-Oliveira (CCB-CFS-UFSC) to the final version of the manuscript. We wish to thank also the excellent and devoted technical assistance and animal care provided by Mr. Eduardo H. Gonçalves, Mr. Carlos H. Espíndola, Mrs. Joanésia M.J. Rothstein, Mr. Emerson V. Fornalski, Mrs. Sandra R B de Oliveira and Mr. Sandro M. de Jesus throughout the experiments.

References

[1] Blundell J. Serotonin manipulations and the structure of feeding-behaviour. Appetite 1986;7(Suppl.):39–56.
[2] Halford J, Wanninayake S, Blundell J. Behavioral satiety sequence (BSS) for the diagnosis of drug action on food intake. Pharmacol Biochem Behav 1998;61(2):159–68.
[3] Rodgers R, Holch P, Tallet A. Behavioural satiety sequence (BSS): separating wheat from chaff in the behavioural pharmacology of appetite. Pharmacol Biochem Behav 2010;97(1):3–14.
[4] Canello M, Ravazio MR, Paschoalini MA, Marino-Neto J. Food deprivation- vs. intraventricular adrenaline-induced feeding and postprandial behaviors in the pigeon (*Columba livia*). Physiol Behav 1993;54(6):1075–9.
[5] Dario AJ, Lopes PR, Freitas CG, Paschoalini MA, Marino-Neto J. Electrographic patterns of postprandial sleep after food deprivation or intraventricular adrenaline injections in pigeons. Brain Res Bull 1996;39(4):249–54.
[6] Spudeit WA, Sulzbach NS, BITTENCOURT MDEA, DUARTE AM, LIANG H, Lino-de-Oliveira C, et al. The behavioral satiety sequence in pigeons (*Columba livia*). Description and development of a method for quantitative analysis. Physiol Behav 2013;122(62–71):2013.
[7] De Vry J, Schereiber R. Effects of selected serotonin 5-HT1 and 5-HT2 receptor agonists on feeding behavior: possible mechanisms of action. Neurosci Biobehav 2000;24(3):341–53.
[8] Güntürkün O, Grothues A, Hautkappe A, Visé F, Wawrzyniak N, Zwilling U. Serotonergic modulation of ingestive behavior in pigeons. Pharmacol Biochem Behav 1989;32(2):415–20.
[9] Steffens SM, Casas DC, Milanez BC, Freitas CG, Paschoalini MA, Marino-Neto J. Hypophagic and dipsogenic effects of central 5-HT injections in pigeons. Brain Res Bull 1997;44(6):681–8.
[10] Da Silva RA, Da Silva AS, Poffo MJ, Ribas DC, Faria MS, Marino-Neto J, et al. Feeding behavior after metergoline or GR-46611 injections into the paraventricular nucleus of the hypothalamus in the pigeon. Behav Brain Res 2007;179(2):248–57.
[11] Brun S, da Luz V, Fernandez M, Paschoalini MA, Marino-Neto J. Atypical angiotensin receptors may mediate water intake induced by central injections of angiotensin II and of serotonin in pigeons. Regul Pept 2001;98(3):127–35.
[12] Dos Santos TS, Meneghelli C, Hoeller AA, Paschoalini MA, Arckens L, Lino-de-Oliveira C, et al. Behavioral profile and Fos activation of serotonergic and non-serotonergic raphe neurons after central injections of serotonin in the pigeon (*Columba livia*). Behav Brain Res 2011;220(1):173–84.
[13] Hoeller AA, Dos Santos TS, Bruxel RR, Dallazen AR, Silva HTA, André ES, et al. Serotonergic control of ingestive and post-ingestive behaviors in pigeons (*Columba livia*): the role of 5-HT1A receptor-mediated central mechanisms. Behav Brain Res 2013;236(1):118–30.
[14] Häckl LPN, Richter GO, Faria MS, Paschoalini MA, Marino-Neto J. Behavioral effects of 8-OH-DPAT injections into pontine and mesencephalic areas containing 5-HT-immunoreactive perikarya in the pigeon. Brain Res 2005;1035(2):154–67.
[15] Portas C, Bjorvatn B, Ursin R. Serotonin and the sleep/wake cycle: special emphasis on microdialysis studies. Prog Neurobiol 2000;60(1):13–35.
[16] Tejada S, Rial RV, Gamundí A, Esteban S. Effects of serotonergic drugs on locomotor activity and vigilance states in ring doves. Behav Brain Res 2011;216(1):238–46.
[17] Jacobs B, Fornal C. Activity of brain serotonergic neurons in the behaving animal. Pharmacol Rev 1991;43(4):563–78.
[18] Monti J. The role of dorsal raphe nucleus serotonergic and non-serotonergic neurons, and of their receptors, in regulating waking and rapid eye movement (REM) sleep. Sleep Med Rev 2010;14(5):319–27.
[19] Koella W, Czicman J. Mechanism of the EEG-synchronizing action of serotonin. Am J Physiol 1966;211(4):926–34.
[20] Bjorvatn B, Fagerland S, Eid T. Sleep/waking effects of a selective 5-HT1A receptor agonist given systemically as well as perfused in the dorsal raphe nucleus in rats. Brain Res 1997;770(1–2):81–8.
[21] Portas CM, Thakkar M, Rainnie D, Mccarley RW. Microdialysis perfusion of 8-hydroxy-2-(di-*n*-propylamino) tetralin (8-OH-DPAT) in the dorsal raphe nucleus decreases serotonin release and increases rapid eye movement sleep in the freely moving cat. J Neurosci 1996;16(8):2820–8.
[22] Gleeson S, Weissman BA, Seggel MR, Barrett JE. Neurochemical effects of 5-HT1 receptor ligands in pigeons. Eur J Pharmacol 1992;229(2–3):109–15.
[23] Mansbach RS, Harrod C, Hoffmann SM, Nader MA, Lei Z, Witkin JM, et al. Behavioral studies with anxiolytic drugs. V. Behavioral and in vivo neurochemical analyses in pigeons of drugs that increase punished responding. J Pharmacol Exp Ther 1988;246(1):114–20.
[24] Bonvento G, Scatton B, Claustre Y, Rouquier L. Effect of local injection of 8-OH-DPAT into the dorsal or median raphe nuclei on extracellular levels of serotonin in serotonergic projection areas in the rat brain. Neurosci Lett 1992;137(1):101–4.
[25] Müller CP, Carey RJ, Huston JP, De Souza Silva MA. Serotonin and psychostimulant addiction: focus on 5-HT1A-receptors. Prog Neurobiol 2007;81(3):133–78.
[26] Sotelo C, Cholley B, El Mestikawy S, Gozlan H, Hamon M. Direct immunohistochemical evidence of the existence of 5-HT1A autoreceptors on serotoninergic neurons in the midbrain raphe nuclei. Eur J Neurosci 1990;2(12):1144–54.
[27] Zilles K, Schleicher A, Glaser T, Traber J, Rath M. The ontogenetic development of serotonin (5-HT1) receptors in various cortical regions of the rat brain. Anat Embryol 1985;172(3):255–64.
[28] Pazos A, Palacios J. Quantitative autoradiographic mapping of serotonin receptors in the rat brain. I. Serotonin-1 receptors. Brain Res 1985;346(2):205–30.
[29] Palchaudhuri M, Flügge G. 5-HT1A receptor expression in pyramidal neurons of cortical and limbic brain regions. Cell Tissue Res 2005;321(2):159–72.
[30] Miquel MC, Doucet IE, Boni AC, El Mestikawy LS, Matthiessen L, Daval G, et al. Central serotonin 1A receptors respective distributions of encoding mRNA, receptor protein and binding sites by in situ hybridization histochemistry, radioimmunohistochemistry and autoradiographic mapping in the rat brain. Neurochem Int 1991;19(4):453–65.
[31] Collin M, Backberg M, Onnestam K, Meister B. 5-HT1A receptor immunoreactivity in hypothalamic neurons involved in body weight control. NeuroReport 2002;13(7):945–51.

[32] Marvin E, Scrogin K, Dudás B. Morphology and distribution of neurons expressing serotonin 5-HT1A receptors in the rat hypothalamus and the surrounding diencephalic and telencephalic areas. J Chem Neuroanat 2010;39(4):235–41.
[33] Herold C, Palomero-Gallagher, A N, Güntürkün O, Zilles K. Serotonin 5-HT1A receptor binding sites in the brain of the pigeon (*Columba livia*). Neuroscience 2012;200:1–12.
[34] Fletcher A, Cliffe I, Dourish C. Silent 5-HT1A receptor antagonists: utility as research tools and therapeutic agents. Trends Pharmacol Sci 1993;14(12):41–8.
[35] Forster EA, Cliffe IA, Bill DJ, Dover GM, Jones D, Reilly Y, et al. A pharmacological profile of the selective silent 5-HT1A receptor antagonist, WAY-100635. Eur J Pharmacol 1995;281(1):81–8.
[36] Monti JM, Jantos H, Silveira R, Reyes-Parada M, Scorza C, Prunell G. Depletion of brain serotonin by 5,7-DHT: effects on the 8-OH-DPAT-induced changes of sleep and waking in the rat. Psychopharmacology (Berl) 1994;115(1–2):273–7.
[37] Alesci R, Bagnoli P. Endogenous levels of serotonin and 5-hydroxyindoleacetic acid in specific areas of the pigeon CNS: effects of serotonin neurotoxins. Brain Res 1988;450(1–2):259–71.
[38] Vergé D, Daval G, Marcinkiewicz M, Patey A, El Mestikawy S, Gozlan H, et al. Quantitative autoradiography of multiple 5-HT1 receptor subtypes in the brain of control or 5,7-dihydroxytryptamine-treated rats. J Neurosci 1986;6(12):3474–82.
[39] Pranzatelli M, Durkin M, Barkai A. Quantitative autoradiography of 5-hydroxytryptaminela binding sites in rats with chronic neonatal 5,7-dihydroxytryptamine lesions. Dev Brain Res 1994;80(1–2):1–6.
[40] Currie P, Coscina D, Fletcher P. Reversal of fenfluramine and fluoxetine anorexia by 8-OH-DPAT is attenuated following raphe injection of 5,7-dihydroxytryptamine. Brain Res 1998;800(1):62–8.
[41] Choi M, Jonak E, Fernstrom J. Serotonin reuptake inhibitors do not prevent 5,7-dihydroxytryptamine-induced depletion of serotonin in rat brain. Brain Res 2004;1007(1–2):19–28.
[42] Ison M, Fachinelli C, Rodriguez Echandia E. Effect of the i.c.v. injection of 5,7-di-hydroxytryptamine on the aggressive behavior of dominant and submissive pigeons (*Columba livia*). Pharmacol Biochem Behav 1996;53(4):951–5.
[43] Mokrosz MJ, Chojnacka-Wójcik E, Tatarczyńska E, Klodzińska A, Filip M, Boksa J, et al. 1-(2-Methoxyphenyl)-4-[(4-succinimido) butyl] piperazine (MM-77): a new, potent, postsynaptic antagonist of 5-HT1A receptors. Med Chem Res 1994;4:161–9.
[44] Karten H, Hodos W. A stereotaxic atlas of the brain of the pigeon (*Columba livia*). Baltimore: Johns Hopkins Press; 1967.
[45] Alfredo B, Picazo O. Effect of the postsynaptic 5-HT1A receptor antagonist MM-77 on stressed mice treated with 5-HT1A receptor agents. Eur J Pharmacol 2005;508(1–3):155–8.
[46] Meneghelli C, Rocha NH, Mengatto V, Hoeller AA, Santos TS, Lino-De-Oliveira C, et al. Distribution of tryptophan hydroxylase-immunoreactive neurons in the brainstem and diencephalon of the pigeon (*Columba livia*). J Chem Neuroanat 2009;38(1):34–46.
[47] Kuenzel W, Van Tienhoven A. Nomenclature and location of avian hypothalamic nuclei and associated circumventricular organs. J Comp Neurol 1982;206(3):293–313.
[48] Reiner A, Perkel DJ, Bruce LL, Butler AB, Csillag A, Kuenzel W, et al. Revised nomenclature for avian telencephalon and some related brainstem nuclei. J Comp Neurol 2004;473(3):377–414.
[49] Crispim Junior C, Pederiva CN, Bose RC, Garcia VA, Lino-De-Oliveira C, Marino-Neto J. ETHOWATCHER: validation of a tool for behavioral and video-tracking analysis in laboratory animals. Comput Biol Med 2012;42(2):257–64.
[50] Da Silva E, Dos Santos TV, Hoeller AA, Dos Santos TS, Pereira GV, Meneghelli C, et al. Behavioral and metabolic effects of central injections of orexins/hypocretins in pigeons (*Columba livia*). Regul Pept 2008;147(1–3):9–18.
[51] Arvidsson LE, Hacksell U, Nilsson JL, Hjorth S, Carlsson A, Lindberg P, et al. 8-Hydroxy-2-(di-*n*-propylamino-)tetralin, a new centrally acting 5-hydroxytryptamine receptor agonist. J Med Chem 1981;24(8):921–3.
[52] Hjorth S, Carlsson A, Buspirone:. Effects on central monoaminergic transmission – possible relevance to animal experimental and clinical findings. Eur J Pharmacol 1982;83(3–4):299–303.
[53] Zilles K, Schleicher A, Palomero-Gallagher N, Amunts K. Quantitative analysis of cyto- and receptor architecture of the human brain. In: Toga A, Mazziotta J, editors. Brain mapping: the methods, 21, 2nd. ed. San Diego: Academic Press; 2002. p. 573–602.
[54] Zilles K, Palomero-Gallagher N, Grefkes C, Scheperjans F, Boy C, Amunts K, et al. Architectonics of the human cerebral cortex and transmitter receptor fingerprints: reconciling functional neuroanatomy and neurochemistry. Eur Neuropsychopharmacol 2002;12(6):587–99.
[55] Schleicher A, Palomero-Gallagher N, Morosan P, Eickhoff SB, Kowalski T, De Vos K, et al. Quantitative architectural analysis: a new approach to cortical mapping. Anat Embriol (Berl) 2005;210(5–6):373–86.
[56] Linder AE, Diaz J, NI W, Szasz T, Burnett R, Watts SW. Vascular reactivity, 5-HT uptake, and blood pressure in the serotonin transporter knockout rat. Am J Physiol Heart Circ Physiol 2008;294(4):H1745–52.
[57] Merker B. Silver staining of cell bodies by means of physical development. J Neurosci Methods 1983;9(3):235–41.
[58] Gozlan H, Elmestikawy S, Pichat L, Glowinski J, Hamon M. Identification of presynaptic serotonin autoreceptors using a new ligand: 3H-PAT. Nature 1983;305(5930):140–2.
[59] Boess F, Martin I. Molecular biology of 5-HT receptors. Neuropharmacol 1994;33(3–4):275–317.
[60] Hoyer D, Clarke DE, Fozard JR, Hartig PR, Martin GR, Mylecharane EJ, et al. International Union of Pharmacology classification of receptors for 5-hydroxytryptamine (serotonin). Pharmacol Rev 1994;46(2):157–63.
[61] Zilles K. Evolution of the human brain and comparative cyto- and receptor architecture. In: Dehaene S, Duhamel S, Hauser JR, Rizzolatti M, editors. From monkey brain to human brain. 2005. p. 41–56.
[62] Zilles K, Bacha-Trams M, Palomero-Gallagher N, Amunts K, Friederici AD. Comon molecular basis of the sentence comprehension network revealed by neurotransmitter receptor fingerprints. Cortex 2015;63:79–89.
[63] Dupuis D, Palmier C, Colpáert FC, Pauwels PJ. Autoradiography of serotonin 5-HT1A receptor-activated G proteins in guinea pig brain sections by agonist-stimulated [35S] GTPyS binding. J Neurochem 1998;70:1258–68.
[64] Simpson MD, Lubman DI, Slater P, Deakin JF. Autoradiography with [3H] 8-OH-DPAT reveals increases in 5-HT (1A) receptors in ventral prefrontal cortex in schizophrenia. Biol Psychiatry 1996;39(11):919–28.
[65] Assié M-B, Koek W. [3H]-8-OH-DPAT binding in the rat brain raphe area: involvement of 5-HT1A and non-5-HT1A receptors. Br J Pharmacol 2000;130(6):1348–52.
[66] To ZP, Bonhaus DW, Eglen RM, Jakeman LB. Characterization and distribution of putative 5-ht7 receptors in guinea-pig brain. Br J Pharmacol 1995;115(1):107–16.
[67] Thomas DR, Middlemiss DN, Taylor SG, Nelson P, Brown AM. 5-CT stimulation of adenylylcyclase activity in guinea-pig hippocampus: evidence for involvement of 5-HT7 and 5-HT1A receptors. Br J Pharmacol 1999;128(1):158–64.
[68] Martín-Cora F, Pazos A. Autoradiographic distribution of 5-HT7 receptors in the human brain using [3H] mesulergine: comparison to other mammalian species. Br J Pharmacol 2004;141(1):92–4.
[69] Bonaventure P, Nepomuceno D, Kwok A, Chai W, Langlois X, Hen R, et al. Reconsideration of 5-hydroxytryptamine (5-HT) 7 receptor distribution using [3H]5-carboxamidotryptamine and [3H]8-hydroxy-2-(di-npropylamino)tetraline: analysis in brain of 5-HT1A knockout and 5-HT1A/1B double-knockout mice. JPET 2002;302:240–8.
[70] Yamada H, Sano Y. Immunohistochemical studies on the serotonin neuron system in the brain of the chicken (*Gallus domesticus*). II. The distribution of the nerve fibers. Biog Amines 1985;2:21–36.
[71] Cozzi B, Viglietti-Panzica C, Aste N, Panzica GC. The serotoninergic system in the brain of the Japanese quail. An immunohistochemical study. Cell Tissue Res 1991;263(2):271–84.
[72] Challet E, Miceli D, Pierre J, Reperant J, Masicotte G, Herbin M, et al. Distribution of serotonin-immunoreactivity in the brain of the pigeon (*Columba livia*). Anat Embryol (Berl) 1996;193(3):209–27.
[73] Hirunagi K, Hasegawa M, Vígh B, Vígh-Teichmann I. Immunocytochemical demonstration of serotonin-immunoreactive cerebrospinal fluid-contacting neurons in the paraventricular organ of pigeons and domestic chickens. Prog Brain Res 1992;91:327–30.
[74] Reiner A, Karle EJ, Anderson KD, Medina L. Catecholaminergic perikarya and fibers in the avian nervous system. In: Smeets W, Reiner A, editors. Phylogeny and development of catecholamine systems in the CNS of vertebrates. Cambridg: Cambridge University Press; 1994. p. 135–81.
[75] Mello C, Pinaud R, Ribeiro S. Noradrenergic system of the zebra finch brain: immunocytochemical study of dopamine-*b*-hydroxylase. J Comp Neurol 1998;400(2):207–28.
[76] Palacios J, Probst A, Cortes R. The distribution of serotonin receptors in the human brain: high density of [3H] LSD binding sites in the raphe nuclei of the brainstem. Brain Res 1983;274(1):150–5.
[77] Sprouse J, Aghajanian G. (−)-Propranolol blocks the inhibition of serotonergic dorsal raphe cell firing by 5-HT1A selective agonists. Eur J Pharmacol 1986;128(3):295–8.
[78] Adell A, Carceller A, Artigas F. In vivo brain dialysis study of the somatodendritic release of serotonin in the raphe nuclei of the rat: effects of 8-hydroxy-2-(di-*n*-propylamino) tetralin. J Neurochem 1993;60(5):1673–81.
[79] Kreiss D, Lucki I. Differential regulation of serotonin (5-HT) release in the striatum and hippocampus by 5-HT1A autoreceptors of the dorsal and median raphe nuclei. J Pharmacol Exp Ther 1994;269(3):1268–79.
[80] Adell A, Celada P, Abellan MT, Artigas F. Origin and functional role of the extracellular serotonin in the midbrain raphe nuclei. Brain Res Rev 2002;39(2–3):154–80.
[81] Johnson A, Gartside S, Ingram C. 5-HT1A receptor-mediated autoinhibition does not function at physiological firing rates: evidence from in vitro electrophysiological studies in the rat dorsal raphe nucleus. Neuropharmacology 2002;43(6):959–65.
[82] Bortolozzi A, Amargos-Bosch M, Miklos T, Artigas F, Adell A. In vivo efflux of serotonin in the dorsal raphe nucleus of 5-HT1A receptor knockout mice. J Neurochem 2004;88(6):1373–9.
[83] Nader M, Barret J. Neurochemical changes in pigeon cerebrospinal fluid during chronic administration of buspirone or 8-hydroxy-2-(di-*n*-propylamino)tetralin (8-OH-DPAT). Pharmacol Biochem Behav 1989;32(1):227–32.
[84] Mignot E, Serrano A, Laude D, Elghozi J-L, Dedek J, Scatton B. Measurement of 5-HIAA levels in ventricular CSF (by LCEC) and in striatum (by in vivo

voltammetry) during pharmacological modifications of serotonin metabolism in the rat. J Neural Transm 1985;62(1–2):117–24.
[85] Coscina D, De Rooy E. Effects of intracisternal vs. intrahypothalamic 5,7-DHT on feeding elicited by hypothalamic infusion of NE. Brain Res 1992;579(2):310–20.
[86] Bjorvatn B, Fagerland S, Eid T, Ursin R. Sleep/waking effects of a selective 5-HT1A receptor agonist given systemically as well as perfused in the dorsal raphe nucleus in rats. Brain Res 1997;770:81–8.
[87] Findlay P, Thompson G. The effect of intraventricular injections of noradrenaline, 5-hydroxytryptamine, acetylcholine and tranylcypromine on the ox (*Bos taurus*) at different environmental temperatures. J Physiol 1968;194(3):809–16.
[88] Dourish C, Hutson P, Curzon G. Characteristics of feeding induced by the serotonin agonist 8-hydroxy-2-(di-*n*-propylamino) tetralin (8-OH-DPAT). Brain Res Bull 1985;15(4):377–84.
[89] Bendotti C, Samanin R. 8-Hydroxy-2-(di-*n*-propylamino) tetralin (8-OH-DPAT) elicits eating in free-feeding rats by acting on central serotonin neurons. Eur J Pharmacol 1986;121(1):147–50.
[90] Currie P, Fletcher P, Coscina D. Administration of 8-OH-DPAT into the midbrain raphe nuclei: effects on medial hypothalamic NE-induced feeding. Am J Physiol 1994;266(5 (Pt 2)):R1645–51.
[91] Fletcher A, Bill DJ, Cliffe IA, Forster EA, Jones D, Reilly Y. A pharmacological profile of WAY-100635, a potent and selective 5-HT1A receptor antagonist. Br J Pharmacol 1994;112:91P.
[92] Fletcher A, Forster EA, Bill DJ, Brown G, Cliffe IA, Hartley JE, et al. Electrophysiological, biochemical, neurohormonal and behavioural studies with WAY-100635, a potent, selective and silent 5-HT1A receptor antagonist. Behav Brain Res 1996;73(1–2):337–53.
[93] Wesolowska A, Borycz J, Paluchowska MH, Chojnacka-Wójcik E. Pharmacological analysis of the hypothermic effects of nan-190 and its analogs, postsynaptic 5-HT1A receptor antagonists, in mice. Pol J Pharmacol 2002;54(4):391–9.
[94] Wesolowska A, Paluchowska M, Chojnacka-Wójcik E. Involvement of presynaptic 5-HT1A and benzodiazepine receptors in the anticonflict activity of 5-HT1A receptor antagonists. Eur J Pharmacol 2003;471(1):27–34.
[95] Sano Y, Ueda S, Yamada H, Takeuchi Y, Goto M, Kawata M. Immunohistochemical demonstration of serotonin-containing CSF-contacting neurons in the submammalian paraventricular organ. Histochemistry 1983;77(4):423–30.
[96] Berk M, Butler A. Efferent projections of the medial preoptic nucleus and medial hypothalamus in the pigeon. J Comp Neurol 1981;203(3):379–99.
[97] Korf H, Simon-Oppermann C, Simon E. Afferent connections of physiologically identified neuronal complexes in the paraventricular nucleus of conscious Pekin ducks involved in regulation of salt- and water-balance. Cell Tissue Res 1982;226(2):275–80.
[98] Korf H. Neuronal organization of the avian paraventricular nucleus: intrinsic, afferent, and efferent connections. J Exp Zool 1984;232(3):387–95.
[99] Haida Y, Ubuka T, Ukena K, Tsutsui K, Oishi T, Tamotsu S. Photoperiodic response of serotonin- and galanin-immunoreactive neurons of the paraventricular organ and infundibular nucleus in Japanese quail, *Cortunix cortunix japonica*. Zool Sci 2004;21(5):575–82.
[100] Marley E, Whelan J. Some central effects of 5-hydroxytryptamine in young chickens at and below thermoneutrality. Br J Pharmacol 1975;53(1):37–41.
[101] Fuchs T, Siegel JJ, Burgdorf J, Bingman VP, et al. A selective serotonin reuptake inhibitor reduces REM sleep in the homing pigeon. Physiol Behav 2006;87(3):575–81.
[102] Pyörnillä A, Hissa R. Opposing temperature responses to intrahypothalamic injections of 5-hydroxytryptamine in the pigeon exposed to cold. Experentia 1979;35(1):59–60.
[103] Da Silva RA, De Oliveira ST, Hackl LP, Spilere CI, Faria MS, Marino-Neto J, et al. Ingestive behaviors and metabolic fuels after central injections of 5-HT1A and 5-HT1D/1B receptors agonists in the pigeon. Brain Res 2004;1026(2):275–83.
[104] Campanella LC, Da Silva AA, Gellert DS, Parreira C, Ramos MC, Paschoalini MA, et al. Tonic serotonergic control of ingestive behaviours in the pigeon (*Columba livia*): the role of the arcopallium. Behav Brain Res 2009;205(2):396–405.
[105] D'hondt E, Vermeiren J, Peeters K, Balthazart J, Tlemcani O,., Ball GF, et al. Validation of a new antiserum directed towards the synthetic c-terminus of the FOS protein in avian species: immunological, physiological and behavioral evidence. J Neurosci Methods 1999;91(1–2):31–45.
[106] Simon E, Gerstberger R, Gray D. Central nervous angiotensin II responsiveness in birds. Prog Neurobiol 1992;39(2):179–87.
[107] Kia HK, Miquel M-C, Brisorgueil M-J, Daval G, Riad M, El Mestikawy S, et al. Immunocytochemical localization of serotonin1A receptors in the rat central nervous system. J Comp Neurol 1996;365(2):289–95.
[108] Steffens SM, Da Cunha IC, Beckman D, Lopes AP, Faria MS, Marino-Neto J, et al. The effects of metergoline and 8-OH-DPAT injections into arcuate nucleus and lateral hypothalamic area on feeding in female rats during the estrous cycle. Physiol Behav 2008;95(3):484–91.
[109] Steffens S, Beckman D, Faria MS, Marino-Neto J, Paschoalini MA. WAY100635 blocks the hypophagia induced by 8-OH-DPAT in the hypothalamic nuclei. Physiol Behav 2010;99(5):632–7.
[110] López-Alonso V, E, Mancilla-Díaz JM, Rito-Domingo M, González-Hernández B, Escartín-Pérez RE. The effects of 5-HT1A and 5-HT2C receptor agonists on behavioral satiety sequence in rats. Neurosci Lett 2007;416(3):285–8.
[111] Aghajanian G, Gallager D. Raphe origin of serotonergic nerves terminating in the cerebral ventricles. Brain Res 1975;88(2):221–31.
[112] Chan-Palay V. Serotonin axons in the supra- and subependymal plexuses and in the leptomeninges; their roles in local alterations of cerebrospinal fluid and vasomotor activity. Brain Res 1976;102(1):103–30.
[113] Simpson KL, Fisher TM, Waterhouse BD, Lin RCS. Projection patterns from the raphe nuclear complex to the ependymal wall of the ventricular system in the rat. J Comp Neurol 1998;399(1):61–72.
[114] Vígh B, et al. The system of cerebrospinal fluid-contacting neurons. Its supposed role in the nonsynaptic signal transmission of the brain. Histol Histopathol 2004;19(2):607–28.
[115] Vigh-Teichmann I, Vígh B. The system of cerebrospinal fluid-contacting neurons. Its supposed role in the nonsynaptic signal transmission of the brain. Arch Histol Cytol 1989;52(Suppl.):195–7.
[116] Danguir L, et al. LCEC monitoring of 5-hydroxyindolic compounds in the cerebrospinal fluid of the rat related to sleep and feeding. Brain Res Bull 1982;8(3):293–7.
[117] Hurtson P, et al. Monitoring 5HT metabolism in the brain of the freely moving rat. Ann N Y Acad Sci 1986;473:321–36.
[118] Johnson A, Gross P. Sensory circumventricular organs and brain homeostatic pathways. FASEB J 1993;7(8):678–86.
[119] Castillo-Ruiz A, et al. Day-night differences in neural activation in histaminergic and serotonergic areas with putative projections to the cerebrospinal fluid in a diurnal brain. Neuroscience 2013;250:352–63.
[120] Parent A. Comparative anatomy of the serotoninergic systems. J Physiol 1981;77(2–3):147–56.
[121] Azmitia E. Serotonin and brain: evolution, neuroplasticity, and homeostasis. Int Rev Neurobiol 2007;(77):31–56.
[122] Norton W, Folchert A, Bally-Cuif L. Comparative analysis of serotonin receptor (HTR1A/HTR1B families) and transporter (slc6a4a/b) gene expression in the zebrafish brain. J Comp Neurol 2008;511(4):521–42.